TAMPEREEN TEKNILLINEN YLIOPISTO
TAMPERE UNIVERSITY OF TECHNOLOGY

MIKKO KIVENTO

NUMERICAL EVALUATION OF SPECIFIC ABSORPTION RATE WITH TWO REALISTIC MOBILE PHONE MODELS

Master of Science thesis

Examiners: prof. Jukka Lekkala, prof. Jari Hyttinen
Supervisor: adj. prof. Jafar Keshvari
Examiners and topic approved by the Faculty Council of the Faculty of Natural Sciences on 8th Oct 2014

ABSTRACT

MIKKO KIVENTO: Numerical evaluation of Specific Absorption Rate with two realistic mobile phone models
Tampere University of technology
Master of Science Thesis, 61 pages, 11 Appendix pages
May 2015
Master's Degree Programme in Bioengineering
Major: Biomeasurements
Examiners: Professor Jukka Lekkala, Professor Jari Hyttinen
Supervisor: Adjunct professor Jafar Keshvari (Aalto University)

Keywords: specific absorption rate (SAR) compliance assessment, specific anthropomorphic mannequin (SAM), microwave radiation, numerical dosimetry

The electromagnetic (EM) energy absorption of human tissues induced by mobile devices is measured in terms of specific absorption rate (SAR), which can also be expressed as the rate of temperature change in time.

IEEE C95 standard and ICNIRP guidelines set exposure limits for occupational environment and general public. The limit for general public is 2 W/kg and for occupational workers 10 W/kg over 6 minutes averaged over 10 g of tissue. The measurement procedures to comply with these limits are described in IEEE 1528 and IEC 62209 standards, where specific anthropomorphic mannequin (SAM) phantom is used for conservative RF exposure assessment. In addition to the measurements, mobile phone radiation may also be assessed numerically using computer aided design (CAD) models, solving EM field calculations in a grid of modelled parts defined with different physical properties.

This thesis is a numerical evaluation of SAR compliance assessment with realistic exposure conditions using accurate human and mobile phone models. Four hand models with four adult and five child head models were simulated with two accurate Nokia mobile phone models, 6630 and 8310, which are more complex in comparison to many of the simpler generic phone models used in other studies. In total over 400 simulations were run with comparable settings to achieve possibility to consider different aspects appearing in the results.

The conclusions in this thesis are in line with the overall conclusions in the RF exposure assessment research. No systematic differences between models are observed, however some differences between different anatomical models, which in some cases seem to be related to the distance of the source and tissues in the cheek area, are observed. The SAR results are clearly dependent on the phone model i.e. the EM field source of the simulation. Most of the differences seen in the results are also related to the hand holding the device. Overall we observe attenuation of the SAR values in the presence of the hand, and with some small number of cases the SAR was increased. Our results do generally confirm the SAM phantom conservativeness in the tested configurations. Important observations about phone material assignment and the connection of head and hand voxels in the simulation domain were made during the process, which provides fundamental knowledge about numerical modeling of realistic mobile phone exposure scenarios.

TIIVISTELMÄ

MIKKO KIVENTO: Ominaisabsorptionopeuden numeerinen arviointi kahdella realistisella matkapuhelinmallilla
Tampereen teknillinen yliopisto
Diplomityö, 61 sivua, 11 liitesivua
Toukokuu 2015
Biotekniikan diplomi-insinöörin tutkinto-ohjelma
Pääaine: Biomittaukset
Tarkastajat: professori Jukka Lekkala, professori Jari Hyttinen
Ohjaaja: dosentti Jafar Kashvari (Aalto-yliopisto)

Avainsanat: ominaisabsorptionopeus (SAR), spesifinen andropomorfinen mannekiini (SAM), mikroaaltosäteily, numeerinen dosimetria

Matkapuhelimen säteilemän sähkömagneettisen säteilyn energian absorptiota ihmisen kudoksiin mitataan ominaisabsorptionopeutena (SAR), joka voidaan ilmoittaa myös käyttäen lämpötilan muutosta ajan suhteen.

IEEE C95 –standardi ja ICNIRPin suositukset määrittelevät altistusrajat ammatillisessa ja tavallisessa käyttöympäristössä. Tavallisessa (valvomattomassa) käytössä raja on 2 W/kg ja ammatillisessa 10 W/kg kuuden minuutin aikana 10 g kudosmassan keskiarvona. Mittaustavat, joilla rajoitusten noudattaminen osoitetaan, on kuvattu mittastandardeissa IEEE 1528 ja IEC 62209, joissa käytetään spesifistä antropomorfista mannekiinia (SAM) konservatiivisessa radiosäteilyn altistusarvioinnissa. Mittausten lisäksi matkapuhelimen säteilyä voidaan tutkia tietokoneavusteisen mallinnuksen (CAD) avulla ohjelmistolla, joka pystyy simuloimaan sähkömagneettisen kentän voimakkuuden ruudukossa, johon on sijoitettu fysikaalisilta ominaisuuksiltaan määriteltyjä kohteita.

Tässä diplomityössä tarkastellaan SAR-arvojen numeerista määrittämistä realistisessa altistustapauksessa käyttäen tarkkoja ihmisen ja matkapuhelimen malleja. Neljää eri käsimallia tutkitaan neljän aikusen ja viiden lapsen päämallin kanssa kahdella tarkasti mallinnetulla Nokian matkapuhelimella, malleilla 6630 ja 8310. Ne ovat huomattavasti tarkempia kuin useissa tutkimuksissa käytetyt geneeriset matkapuhelinmallit. Yhteensä yli 400 vertailukelpoisilla asetuksilla suoritettua simulaatiota mahdollistavat useiden eri tekijöiden analysoinnin saaduista tuloksista.

Tehdyt johtopäätökset vastaavat muita alan tutkimuksia. Emme löytäneet systemaattisia eroja mallien välillä, mutta havaitsimme eri anatomisten mallien kesken eroavuuksia, jotka näyttäisivät liittyvän säteilylähteen etäisyyteen ja posken alueen kudosten koostumukseen. SAR-tulokset ovat selvästi puhelimesta eli sähkömagneettisen kenttäsimulaation lähteestä riippuvaisia. Suurin osa eroavuuksista tuloksissa johtuu ainakin osittain käden vaikutuksesta säteilyn jakautumiseen. Havaitsimme pääasiassa SAR-arvojen heikkenemistä käden ollessa läsnä simulaatiossa, sekä muutaman tapauksen, joissa SAR-tulos voimistui. Tulokset vahvistavat kuitenkin SAM-fantomin yleisen konservatiivisuuden tutkituissa tapauksissa. Lisäksi teimme merkittäviä havaintoja puhelimen materiaalien mallintamisesta sekä käden ja pään kontaktista laskentaruudukossa, jotka antavat tärkeää tietoa matkapuhelimen aiheuttaman altistustilanteen realistisesta numeerisesta mallintamisesta.

PREFACE

This thesis has been written while working for Nokia Corporation Electromagnetic Fields (EMF) Research Team, which upon completion of this thesis has transferred under Microsoft Corporation. The team collaborates closely with the International Electrotechnical Commission (IEC) Technical Committee (TC) 106 Maintenance Team MT1 and Institute of Electrical and Electronics Engineers / International Committee on Electromagnetic Safety (IEEE/ICES) TC34, which are responsible for the development and maintenance of the IEC 62209 and IEEE 1528 series of standards concerning the specific absorption rate (SAR) assessment of mobile wireless communication devices used close to the head or body. Both IEC MT1 and IEEE/ICES TC34 committee members are the foremost experts in the field of EMF near field compliance assessment in the world.

Dr. Jafar Keshvari has been the supervisor of this thesis during the entire project, also working for Nokia and Microsoft. He currently holds an adjunct professorship of Bioelectromagnetics at Aalto University in Helsinki. With the papers and studies related to this thesis we worked with Dr. Andreas Christ, a longtime member of IT'IS foundation and IEC, currently leading the project team for the IEC 62704-1 standard governing the FDTD method. I want to sincerely thank both doctors for their guidance in many topics of my work.

Tampere, 20.5.2015

Mikko Kivento

CONTENTS

LIST OF FIGURES

LIST OF TABLES

LIST OF SYMBOLS AND ABBREVIATIONS

2G, 3G, 4G	generations of mobile telecommunication standards
AIEE	American Institute of Electrical Engineers
ANSI	American National Standards Institute
ASA	American Standards Association
BMI	body mass index
BR	basic restrictions
CAD	computer-aided-design
CE	European Conformity declaration
CENELEC	European Committee for Electrotechnical Standardization
CTIA	The Wireless Association (earlier Cellular Telecommunications Industry Association)
DPP	distance to pivot plane
DUT	device under test
EEC	ear entrance canal
EF	European female
EM	electromagnetic
EMF	electromagnetic field
EN	European Standard
ERP	ear reference point
EU	European Union
FDIS	final draft international standard
FDTD	Finite-Difference Time-Domain method
GPU	graphics processing unit
GSM	Global System for Mobile Communications
ICES	International Committee on Electromagnetic Safety
ICNIRP	International Commission on Non-Ionizing Radiation Protection
IEC	International Electrotechnical Commission
IEE	British Institution of Electrical Engineers
IEEE	Institute of Electrical and Electronics Engineers
IQR	interquartile range
IRE	Institute of Radio Engineers
IRPA	International Radiation Protection Association
IT'IS	The Foundation for Research on Information Technologies in Society
LTE	long-term evolution, also marketed as 4G LTE
M	mouth point
MCells	millions of cells (voxels)
MPE	maximum permissible exposure
MRI	magnetic resonance imaging
MT	maintenance team
NC	national committee
NF-line	neck-front line
PDA	personal digital assistant
PEC	perfect electric conductor
psSAR	peak spatial-average specific absorption rate
PT	project team
RF	radio frequency

RPD	reference plane down
RPU	reference plane up
SAM	specific anthropomorphic mannequin
SAR	specific absorption rate
SC	subcommittee
SCC	standards coordinating committee
SFS	Finnish Standards Association
T	tangent point
TC	technical committee
TP	tangent plane
UMTS	Universal Mobile Telecommunications System
UV	ultraviolet
VF	Virtual Family
VHM	Visible Human Male
WCDMA	Wideband Code Division Multiple Access
WG	working group
WLAN	wireless local area network

c	speed of light
c	specific heat capacity
$\mathbf{E}$	electric field
$\mathbf{H}$	magnetic field
J	current density
m	mass
P	power
S	power density
T	time period
ε_r	relative permittivity
ρ	volumetric mass density
σ	conductivity

1. INTRODUCTION AND OBJECTIVES

According to Official Statistics of Finland, the amount of smart phone users in Finland has risen from 50 to 60 % during year 2014. The same statistics show that in the past three months before the survey, 88 % of 16-24 year old citizens used an instant messaging service with a mobile phone. [1] Already in June 2012, the total ratio of households owning a mobile phone was found to be 98 %. [2] Even more interesting numbers are available at GSMA Intelligence, where Q4 of 2014 statistics show that there are 10.2 million mobile subscriptions in Finland, still growing by 2 % per year. This means that there are 1.86 subscriptions per every 5.5 million Finnish citizens. 77 % of these are broadband connections, in other words 3G or 4G. [3]

The basic function of a modern mobile phone is based on two-way broadcasting and receiving of electromagnetic (EM) radio signals in microwave frequency band between the handset and the telephone operators' relay stations. This means that when using the phone in the traditional way, holding it against the ear, the transmitting antenna of the device is somewhere near the head tissues. Most of the time, when not used actively, the phone makes only very short contacts with the base stations and thus the radiation exposure remains almost unnoticeable over time. Only when the active transmission e.g. a phone call is in effect, the phone radiates continuously (in a cyclic fashion). [4]

There are two organizations that have set the actual limits for the exposure in their documents, which are the ICNIRP Guidelines and IEEE C95.1 standard. On the other hand there are the measurement reference documents like IEEE 1528 and IEC 62209-1 describing measurement methods. In short explanation, the limits given as specific absorption rate (SAR) are decided according to laboratory and field observations of the exposure and multiplied by safety factors for the general public. The measurement documents are meant to unify the testing of radiating devices so that all the testing facilities apply the same methods and conventions in such way that the measurement results are comparable and they can be used to demonstrate the compliance of the limits.

The methods to evaluate the SAR are based on the usage of specific anthropomorphic mannequin (SAM) phantom. The phantom is filled with a liquid corresponding human head tissue values in electromagnetic field and probed with a measurement device while the tested phone is radiating next to the phantom. Since the laboratory measurements require time and material, another way of evaluating the effects has lately been given a lot of interest. The development of powerful computers and computational tools has made the simulation of EM fields fast, cheap and increasingly accurate option. For around 20 years, different computational studies have been evaluating the SAR in hu-

man models based on realistic anatomical data from e.g. magnetic resonance imaging. These simulations can in many ways be seen to be more interesting than the phantom measurements, since by using realistic phone models and adding an anatomically correct hand, the simulated situation is in many ways closer to the realistic mobile phone use. Large scale measurements of human subjects and especially the field values inside the head tissues would be very difficult in the magnitude that can be achieved with easily repeatable numerical simulations.

Very recently, the measurement standard IEC 62209-1 has been updated after years of studying of different effects on SAR. For example a multiple-phase SAM Conservativeness study with international inter-laboratory comparisons of both simulations and reference measurements was conducted with realistic head and hand models of different age and gender, simulated with multiple different phone models in frequencies from hundreds of MHz to a few GHz. The word "conservativeness" refers to the goal to see if the SAM phantom maintains its definition, giving as high or higher SAR results in the tested situations compared to these other models.

The effect of a realistic hand in the simulation domain has been shown to be very complex, giving both lower and higher SAR results in comparison to the situation without hand, which is close to the laboratory setup, where the device is held against the phantom with a lossless device holder. What the phantom measurements also do not show, is whether the size of the head under the exposure affects to the results, i.e. if there are differences between adults and children under the same conditions.

This thesis is based on the SAM Conservativeness studies and will partly use the same protocol as the one used in the interlaboratory comparisons. The 4 hand models from that project are simulated with 4 adult and 5 child head models to widen the scope of different head models used earlier. The transmitters used as sources of the EM field are two accurate Nokia mobile phone models, 6630 and 8310, which are more complex in comparison to many of the simpler generic phone models used in other studies. In total over 400 simulations were run with comparable settings to achieve possibility to consider different aspects appearing in the results. The SAR results data is analyzed to study at least the following questions:

- Is the SAR exposure dependent on head size? Values of adults and children will be compared separately to assess the difference.
- How does a hand holding the mobile phone affect the SAR values? Studies have observed both enhancement and reduction of SAR when the hand is present in the simulation. SAR values with no hand present will be compared to the simulations with specific grips for adults and children holding the device to evaluate the effect.
- Is the SAM phantom conservative in the studied cases and configurations? That is, are the SAR values of the studied Nokia devices with the studied head and

hand models lower than the SAR values simulated with the SAM phantom in the measurement setup of the standards?

The large number of cases with accurate models gives opportunity to find credible similarities and differences but also important artifacts and details caused by the choices made in the modeling and simulations, which will help evaluating the importance of computational results and give ideas for the future studies of SAR.

2. THEORETICAL BACKGROUND

In this chapter we establish the background for the reader to be able to follow the materials and methods presented in this study. The very first topic is naturally the electromagnetic fields, more precisely the part of the electromagnetic spectrum that is used for radio communications and thus concerns our study of mobile phone SAR. The most relevant background of the SAR itself is introduced in the second part of this chapter. Additional to the equations, the backgrounds for the evaluation of SAR and for the exposure limits are shown.

At the end of this chapter, a section explaining the measurement methods of SAR is provided. This includes the most important official standards that govern the laboratory procedures and regulate the test conditions and reporting.

2.1 Electromagnetic fields

The different possible wavelengths of electromagnetic (EM) waves, or in other words the frequencies in which they are observed, are generally referred to as the electromagnetic spectrum. At least frequencies from 1 to 10^{24} Hz have been detected. These waves share some important properties, such as the propagation speed in vacuum, c = 299792458 m/s. The ranges of EM waves are called with different names according to their known properties. Most commonly we observe the visible light (400-700 nm or 750 to 430 THz). Below these frequencies there are infrared, microwaves and radio waves, above there are ultraviolet (UV), X-rays and gamma rays. Table 1 gives the known properties of different frequencies in practical terms. [4] [5]

Table 1. *Descriptions and properties of EM fields.*

Frequency band	Field description	Field properties
Under 30 MHz	Quasi-static. Wavelength in meters.	Radiation is penetrating everywhere by induction of whole-body electric field.
30-3000 MHz	Resonance frequencies. Wavelength is close to the body dimensions.	Due to the convenient wavelength, inner body parts may resonate with the field and absorb the energy.
Over 3 GHz	Wavelength is short in comparison to the tissues.	Surface tissues consume most of the energy. Penetration is small.
400-800 THz	Visible light. Wavelength in nanometers.	Radiation affects only the surface tissues.

Over 800 THz	UV, X-rays, gamma rays. Wavelength is in atomic dimensions.	Radiation becomes highly penetrating and ionizing, liberating electrons.

The radio waves are roughly between 3 kHz and 1 GHz (or 1000 MHz) and microwaves from 1 GHz to 300 GHz. Sometimes both of these ranges are called radio frequencies (RF) [4] [5]. These are also the frequencies we are particularly interested in, and they are part of the spectrum called non-ionizing radiation. To be more exact, the cellular telecommunication i.e. the operating frequencies of mobile phones are in the range of 380 – 2700 MHz. Technologies and frequencies used in Finland are specified in Table 2. [6] [7] [8] [9].

Table 2. *Mobile telecommunication networks and uplink (transmitting) frequencies used in Finland. GSM (Global System for Mobile Communications), UMTS (Universal Mobile Telecommunications System), LTE (Long-Term Evolution) according to generations (2G, 3G and 4G).*

Generation	Technologies	Frequencies (MHz)
2G	GSM 900	890 - 915
	GSM 1800	1710 - 1785
3G	UMTS 900	880 - 915
	UMTS 2100	1920 - 1980
4G	LTE 1800	1710 - 1785
	LTE 2600	2500 - 2570

Electromagnetic waves are described by Maxwell's equations (2.1)-(2.4), which show that the time-varying electric field acts as a source of a magnetic field and the time-varying magnetic field acts as a source of an electric field. These equations are otherwise known as Faradays law of induction (2.1), Ampere's circuital law with Maxwell's addition (2.2), Gauss's law (2.3) and Gauss's law for magnetism (2.4). The opposite for these would be the static fields, for example the electric field of a charge at rest or the magnetic field of a steady current. In our following considerations, we are mainly concerned about the propagating EM fields, also known as radiation. [4] [5]

$$\nabla \times \boldsymbol{E} = -\frac{\partial(\mu \boldsymbol{H})}{\partial t} \tag{2.1}$$

$$\nabla \times H = \frac{\partial(\varepsilon E)}{\partial t} + J \tag{2.2}$$

$$\nabla \cdot \varepsilon E = \rho \tag{2.3}$$

$$\nabla \cdot B = 0 \tag{2.4}$$

2.2 Specific absorption rate and exposure standards

Since the 1960 initiated Radiation Hazards Standards project of American Standards Association (ASA), the Department of the Navy and the Institute of Electrical and Electronics Engineers (IEEE), the radio frequency (RF) standards have been under development in various standard institutions. The first national RF standard was published in United States in 1966 with the name C95.1-1966. It was based on simple thermal models and only gave a general exposure limit of 10 mW/cm² for the frequency band from 10 MHz to 100 GHz. [10] [11] [12] [13]

ASA was a predecessor for the American National Standards Institute (ANSI), which was formed in 1969. Under ANSI the development of the C95 continued, with versions of 1974 and 1982. The most significant improvement was made in the latter, which has the following definition: "*specific absorption rate (SAR). The time rate at which radio-frequency electromagnetic energy is imparted to an element of mass of a biological body.*" The term was hence adopted as the quantity of the exposure limits and remains the common unit for comparing the EMF effects studies until today. [10] [14]

In the late 80s, the C95 standard development passed under the sponsorship of IEEE. The actual exposure limits remained undecided until the C95 revision of 1991. This revision gave the Maximum Permissible Exposure (MPE) values for the whole body average SAR and the spatial peak SAR (per gram of tissue in the shape of a cube) and extended the frequency range to be from 3 kHz to 300 GHz. Revisions of 1999 and 2005 (current) introduce the concept of basic restrictions (BR) that are limits for the internal fields, from which the MPE limits for the external fields are derived. [11] [12] [15]

The other side of radiation research involving ionizing radiation and biological subjects, known as "Health Physics", had been developing since the Manhattan Project of World War II. At the time of the first C95 standard, the International Radiation Protection Association (IRPA) had recently been established. In 1974 a working group was formed to study also non-ionizing radiation and it worked in cooperation with the Environmental Health Division of World Health Organization until in 1992 an independent International Commission of Non-Ionizing Radiation Protection (ICNIRP) was formed. [16] [17]

ICNIRP worked during the 90s with similar goals that the IEEE had in C95.1. The limitations for electromagnetic field (EMF) exposure were studied and decided according to the reported and observed health effects. The frequency range of time-varying EMF up to 300 GHz is covered and the exposure limits given separately for occupational and general public exposure. This is well comparable with the C95.1, where the limits are discussed for uncontrolled and controlled exposures. However, the importance of ICNIRP Guidelines published in 1998 is in their distinct way of presenting the limits. The BR values are given as SAR, current density (J) and power density (S) values. For con-

venience, because the only measurable property of these is the power density in the air outside the body, also reference levels of e.g. electric and magnetic field strengths and electric currents in the limbs are provided for exposure assessment. These values are more practical to measure and then to use to assess, whether the basic restrictions are likely to be exceeded. When the IEEE C95.1 reached its revision of 2005, these two documents became compatible. [12] [16]

What we are interested in these limits, is the originally ICNIRP Guidelines basic restriction for local SAR in head area between 100 kHz and 10 GHz frequencies for general public, **2 W/kg**, over 6 minutes and averaged over 10 g of tissue. This is the value applied for example in the commercial mobile phone testing. [4] [16]

To briefly mention the origin of mobile phone related standards in Finland, they are inherited from the European Committee for Electrotechnical Standardization (CENELEC), which was formed in the beginning of 1973. It is not directly part of the EU, but is responsible for e.g. European Standards (EN), Harmonization Documents (HD) and CE (European Conformity) marking of products, meaning that they meet the requirements set by the EU legislation. As a member of CENELEC, Finland must give EN standards the status of national standard without alteration. This responsibility lies with an organization named Sesko ry, a member of the Finnish Standards Association (SFS) and one of its standards-writing bodies. Approximately 75 % of the EN standards in turn are directly based on the standards of the International Electrotechnical Committee (IEC), which we will introduce in the next chapter. [18] [19]

2.2.1 Equations and units

To establish a connection from the EM field to the specific absorption rate, we need to take a look at what happens in the air or tissue after the electromagnetic wave leaves the source i.e. phone antenna. Inside the square root in Equation (2.5), we see the basic cosine wave equation for a time-harmonic electric field. The integral is taken over the period T and the amplitude for the field is E. The square root gives us the root mean square (*rms*) value, which is the effective value of the electric field. It can be more easily written as the peak value E divided by $\sqrt{2}$. That is the case for a polarized x-directional wave, but in case we have a more arbitrary electric field, the field value can be combined from the square sum of the components, shown in Equation (2.6).

$$E_x = \sqrt{\frac{\int_T \left[E_{a,x}\cos(\omega t + \theta_x)\right]^2 dt}{T}} = \frac{E_{a,x}}{\sqrt{2}} \tag{2.5}$$

$$E_{rms} = \sqrt{E_{rms,x}^2 + E_{rms,y}^2 + E_{rms,z}^2} \tag{2.6}$$

It can be shown, that in the tissues the effective value defines the power loss in that location and causes the observed temperature rise. The effective magnetic field is calculated similarly, but it does not have as clear physical effects as the E-field. [4]

As indicated by the standards and literature, the widely accepted quantity for demonstrating the dosimetric exposure in frequencies over 100 kHz is the specific absorption rate (SAR). It shows the effect and absorption of EM fields to lossy tissues, meaning that there is power loss in the dielectric medium because of the polarization of molecules and the movement of free electrons. Thus the first way to formulate the quantity is with the absorption of power *dP* to an infinitesimal piece of mass *dm*. Here we can also directly see the unit used for SAR, watts per kilograms (W/kg) or sometimes milliwatts per gram (mW/g) for convenience. [4] [16]

$$SAR = \frac{dP}{dm} = \frac{\sigma {E_i}^2}{\rho} = c\frac{dT}{dt} \tag{2.7}$$

In Equation (2.7) there is also the other ways of calculating the SAR, formulated with the basic properties of e.g. tissue, electrical conductivity (σ), mass density (ρ) and specific heat capacity (c) with the prevailing electric field strength **E** or the temperature increase *dT/dt*. The energy transfer can be observed and measured as the rise of tissue temperature as we discussed earlier with the comparison to the microwave ovens. This equation is also important in the SAR laboratory measurements, where a dielectric medium under EMF exposure is measured with an isotropic probe and the local SAR derived with the equation. In practice the SAR is calculated by averaging a cubical piece of tissue, e.g. in ICNIRP Guidelines the mentioned 10 g cube would be approximately 2.15 x 2.15 x 2.15 cm^3 assuming the density of water, 1000 kg/m^3. [4] [16] [32]

Also computational dosimetry is based on the calculations with these variables, in terms of spatial-peak SAR. This definition is preferred for two main reasons: the maximum SAR on a single point (local SAR) is too sensitive for approximation with computational methods and the energy deposited at a point is invariably smeared out due to heat conduction which implies that local SARs are not thermally significant. The computational method computes SAR at every point of the tissue by averaging the values of a region (R) with a mass (M) in a finite volume (V). This leads to the equations (2.8) and (2.9), where $\boldsymbol{r}_0 \in R$. In the latest SEMCAD, the averaging is conducted according to the standard IEC/IEEE 62704-1, which we will introduce in Chapter 3.1.2. [32]

$$\langle SAR(\boldsymbol{r}_0)\rangle = \frac{1}{M}\int_R SAR(\boldsymbol{r})dm \tag{2.8}$$

$$= \frac{1}{M}\int_R \sigma(\boldsymbol{r})\|\boldsymbol{E}(r)\|^2 dv \tag{2.9}$$

2.3 SAR compliance assessment

Institute of Electrical and Electronics Engineers, IEEE, has its roots far back in 1884, when a group of professionals (such as Thomas Edison and Alexander Graham Bell) formed an organization for electrical engineers to support and share their innovations, named American Institute of Electrical Engineers (AIEE). Later in 1912 a similar institute was formed for radio engineers, named the Institute of Radio Engineers (IRE). These two merged in 1963 to form IEEE, with around 150 000 members, 140 000 of which were in the US. [20]

IEEE has different committees for different scientific areas called standard coordinating committees (SCC), which in turn have subcommittees (SC), which in turn have working groups (WG). Our interest is now in the work of IEEE SCC34 SC2 (Wireless Handset Certification) WG1 (Measurement Techniques) which is an extension of IEEE C95.3 (the committee C95 was adopted under IEEE in the late 80s, refer to Chapter 2.2). The first IEEE/ANSI approved standard version was IEEE Std 1528-2003, "IEEE Recommended Practice for Determining the Peak Spatial-Average Specific Absorption Rate (SAR) in the Human Head From Wireless Communications Devices: Measurement Techniques". The scope of this recommended practice is to specify the protocols and test procedures for the measurement of the peak spatial-average SAR inside a simplified head model, induced by handheld radio transceivers intended to be used for personal wireless communication and held against the ear. [21]

The procedures of this practice are intended to give a conservative estimate of SAR in the significant majority of persons but not to cover every possible case of user and use. Details of instrumentation, calibration and phantoms are provided, but not the specific SAR limits, since these are covered in C95.1 and ICNIRP documents. [21]

An amendment of 1528a-2005 added a CAD file for Human Head Model, also called Specific Anthropomorphic Mannequin (SAM) Phantom, which will be introduced in detail in its own subchapter 2.3.1. The newest draft of 1528-2013 by IEEE ICES TC34 SC1 (SAR evaluation - measurement techniques) has been recently approved as an active standard. [22]

Finally, we get to the International Electrotechnical Commission (IEC), which is considered to be the world leading organization of electrotechnology today. The commission was officially founded in London in 1906, where its headquarters resided until moving to Geneva in 1948. The foundation of the commission was originally proposed by the International Electrotechnical Congress in St. Louis, USA in 1904, to which amongst others attended members from the British Institution of Electrical Engineers (IEE) and the American AIEE. The first president of IEC is probably the most well-known, William Thomson a.k.a. Lord Kelvin, who held the position until his death in 1907.

During the first decades, the work of the commission was focused on harmonization of symbols and nomenclature internationally, which later contributed to the SI system. During the 20th century, more TCs were created according to the new fields of electrotechnology, towards the current number of 97. The one we are interested in, TC106 (Methods for the assessment of electric, magnetic and electromagnetic fields associated with human exposure), was created in October 1999. [23] [24]

The measurement standard IEC 62209-1 ed.1: "Human exposure to radio frequency fields from hand-held and body-mounted wireless communication devices – Human models, instrumentation, and procedures – Part 1: Procedure to determine the specific absorption rate (SAR) for hand-held devices used in close proximity to the ear (frequency range of 300 MHz to 3 GHz)" was approved in 2005. This was an informal cooperation between CENELEC TC106x WG1, IEEE SCC34 and IEC TC106 and the primary effort was to harmonize the standardization work of the IEC project team for 62209 to respect the already published IEEE 1528. [25]

The objective of 62209-1 is to specify the measurement methods for testing the compliance with the SAR limits for mobile devices held against the ear. That is, again the limits are those described in other guidelines. IEC 62209-2 ed. 1: "Human exposure to radio frequency fields from hand-held and body-mounted wireless communication devices – Human models, instrumentation, and procedures – Part 2: Procedure to determine the specific absorption rate (SAR) for wireless communication devices used in close proximity to the human body (frequency range of 30 MHz to 6 GHz)" was published in 2010 in response to the broadening field of use for wireless devices. As the title tells, the frequency range is wider and the standard also covers body-mounted and wearable devices which may be used simultaneously in close proximity to human body. [25] [26]

In the late 2000's, it was indicated by different studies that the SAR induced by a mobile phone may be enhanced by a hand holding the device against the head. IEC 62209 standard maintenance team initiated both measurement and computational studies to examine the hand effect to conclude, whether the standardized procedures including only the SAM phantom and lossless device holder should be revised. Ultimately, the results both confirmed the possibility of the hand effect in certain cases with certain devices, but at the same time proved the vast uncertainty in predicting the hand effect before the measurements. A vote between the national committees (NC) of IEC member countries decided to maintain the current SAM only test protocol, but also to add an informative annex collecting the hand effect research as an additional part of the IEC 62209-1 standard. This means that the IEC 62209-1 ed. 2.0 is about to enter the Final Draft International Standard (FDIS) stage and be published by the end of year 2015. [27]

Additional to the measurements, the compliance to the SAR limits can also be assessed by numerical methods, more closely introduced in Chapter 3.1. This thesis is based on

the numerical evaluation of SAR and the goal is to study the details of the numerical results. However, many aspects related to the numerical methods remain unclear and the current standards are dominated by the measurement methods.

2.3.1 SAM Phantom

United States Army updated their anthropometric i.e. human body dimensions database during the years 1987-1988 to provide itself with data for designing of clothing, protective equipment and workspaces. The raw data of over 180 body dimensions was collected from a total of more than 9000 male and female soldiers. The working database representing the components of both genders was created by stratified random sampling to form a working sample of 1774 males and 2208 females. [28]

The head size considerations in preparation of IEEE 1528 used an approach of designing a phantom in such way that the distance between the handset and liquid was always smaller than in 90 % of the sample population for a given set of handset positions. Using the anthropometric data from the above mentioned U.S. army database, relevant subset of 90-percentile male head data was used to derive SAM phantom dimensions defined by the standard. The standardized shape of the phantom is illustrated in Figure 1. [21]

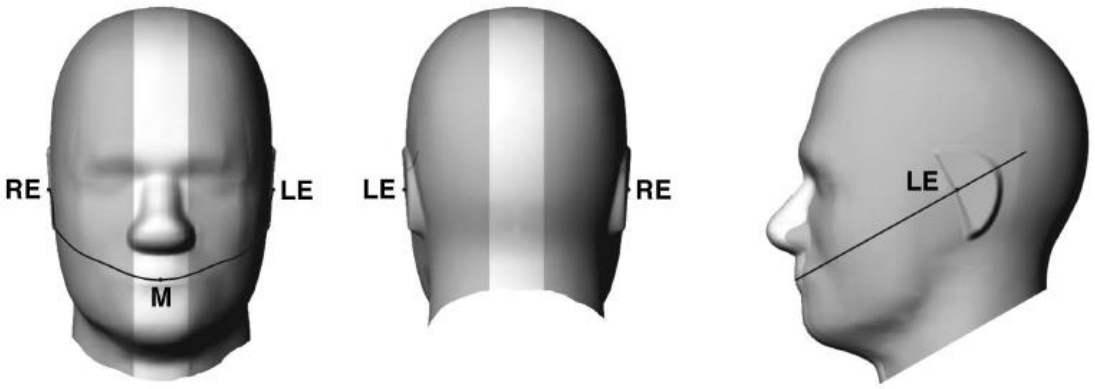

Figure 1. *Front, side and back views of SAM phantom shell model. M is center-of-mouth reference point, LE and RE are left and right ear reference points (ERPs). [21]*

One important exception to the anthropometric data was with the ear of the phantom. Instead of human ear shape the SAM is equipped with an ear spacer, which is considerably less complex and more evenly adapted along the cheek and the side of the head. The pinna (meaning the outer part of the human ear) orientation and shape for SAM were selected to maximize the inductive coupling from the handset. The half-moon shape of the ear spacer is well presented in Figure 1. [21]

Figure 2. *Sagittally bisected phantom halves. Shown placed on their side as used for SAR measurements. Note the perimeter extension for adequate liquid depth. [21]*

Actually in laboratory conditions, the phantom is usually on its side (Figure 2) and split in half, to enable measurements to be conducted in both sides of the head, as the measurement standards dictate. In this setup the SAM may be thought as a pool of the tissue-simulating liquid, in which measurements can be conducted with for example a robotic arm equipped with a probe capable of measuring in three orthogonal axes, isotropically, so that the measurement result gives the actual electric field effective value in the measurement point. The measurements are controlled by a computer, which guides the probing of a precise measurement grid from point to point and collects the E-field data for SAR evaluation. [29] [30]

The tissue-equivalent liquid filling of the phantom volume is based on anatomical variations in the head region behind and above the ear for a cross-section of a representative user population. The dielectric values of the homogeneous liquid for different frequencies were chosen according to the studies to produce the same or slightly higher peak spatial-average SAR in comparison to the highest values occurring in the heterogeneous cases. This aims to satisfy the conservativeness criteria of the SAR assessment, which means that the measurements have to give at least as high dosimetric results as the human tissues would give, or in other words, the measured value will not be less than the expected value during normal use by majority of users. [21] [25] [31]

2.3.2 Device test conditions and reporting

According to IEEE 1528 [21] [22] and IEC 62209-1 [25], "*A SAR measurement system is composed of a phantom, electronic measurement instrumentation, a scanning system and a device holder.*" These documents give detailed specifications on the testing protocols of devices mentioned in the name (i.e. scope) of the standard, respectfully. The basic principles of the protocols are as follows, but multiple exceptions are also covered by the standards.

The device under test (DUT) shall use its internal transmitters and antennas with fully charged battery and equipment specified by the manufacturer, that is, no cables possibly interfering with the measurement should be attached. Two general handset positions,

cheek and “tilt” shall be tested on both left and right sides of the phantom. These are defined to give reliable estimates to the variation of the device position under normal use, provided by the “tilt” position, which means that the phone is rotated 15 degrees outward with the phone acoustic output point remaining in front of the ear. More details on the touch and tilt positions are discussed in Chapter 3.5 with the definition of these positions for anatomical head models.

Not all possible frequency channels of all possible frequency bands need to be tested, but a subset including the center frequency of the band and depending on the width of the band, a collection of other frequencies defined in the protocol. Also the scanning grid details and scanning procedures are given to the SAR distribution and the maximal value measurements. The measurement data is then post-processed and the whole measurement setup and procedures validated (uncertainty evaluation), which is also described in detail for probes, phantoms, test positions etc.

Finally, a test report is generated by collecting all the general data of the device, the laboratory and the testing equipment, detailed uncertainty estimation and test conditions as well as a report summary including the produced SAR values of all the test conditions mentioned above. [21] [22] [25] [26]

3. MATERIALS AND METHODS

This study is heavily dependent on the computer-aided-design (CAD) environments and numerical methods. In this chapter we will first introduce the computational concepts and CAD models of all the parts of our simulations i.e. head models, phone models and hand models. These have been chosen from widely accepted sources and mostly to match the materials in the studies conducted by the IEC 62209-1 maintenance team, which also was the original forum to review the results of this project. The required model manipulations and simulation settings are presented in their own subchapters. At the end of the chapter we have a brief summary of the post processing steps needed for acquiring the actual results.

3.1 Numerical methods

Numerical methods in our context are related to the computational processes of the study. To establish a relation between laboratory measurements and computational results, we have to understand the basics behind these both. We already have discussed the basics of EM fields in Chapter 2.1, especially the importance of the Maxwell's equations. We will now see how they are applied to computational tasks and how the computational procedures are regulated.

3.1.1 Yee cell and Finite-Difference Time-Domain method

The Maxwell's equations (2.1)-(2.4) present the time-varying electric and magnetic fields. Mathematically they are relatively simple first order partial differential equations, which usually can be solved in homogeneous environments with proper knowledge of the initial values, field sources and boundary conditions. However in more complex domain, computational methods are needed. With those, the computational domain is usually divided into smaller boxes called volume pixels or "voxels". These cells are then used in calculations applying Maxwell's equations. [4] [32]

In 1966, Kane Yee published a paper [33] describing the solution of Maxwell's equations in isotropic media. He introduced a procedure of choosing certain field points to form a system called Yee cell (Figure 3), in which the alternating electric (**E**) field (along the edges) and magnetic (**H**) field (along imaginary lines going through the center of the facets) take turns in between each other.

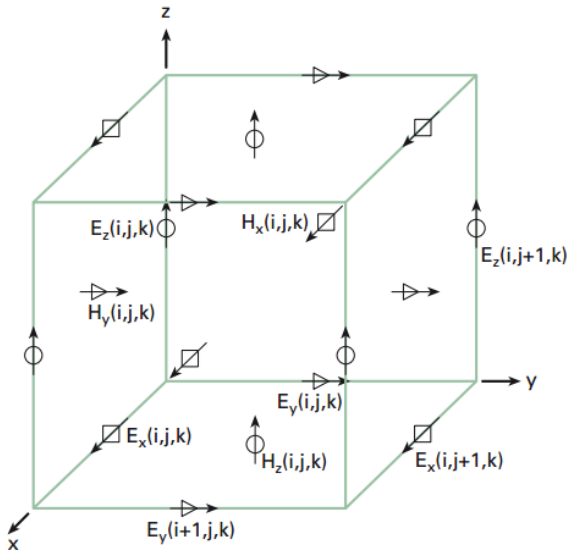

Figure 3. *Yee cell. The alternating electric (**E**) and magnetic (**H**) field components in different axes (x,y,z) noted by coordinate indexes i,j and k. [4]*

It can be seen that every component of both fields is surrounded by components of the other field. This establishes the relation to the Maxwell's curl equations (2.1)-(2.2). The brilliance of this choice of points becomes clear, when the Maxwell's equations are modified into a finite difference equation set of **E** and **H** field operators on a staggered grids in space and time. In 70's and 80's it was shown that a computational domain divided into Yee cells can be calculated using these finite difference equations in the time domain. This implies to a solving method called Yee algorithm, where the Maxwell's equations of one time point consist of **E** and **H** values of the next time point, alternating between the **E** and **H** fields in a manner referred to as leapfrog integration. The term and acronym FDTD for the method was originally used by Allen Taflove in his book about the topic in 1980. [4] [32] [33] [34]

3.1.2 IEC/IEEE 62704-1

The IEC and IEEE have been introduced shortly in Chapter 2.3. We now look at the draft standard written by one of the project teams of the IEC TC106, which also has the maintenance team of 62209-1 among its suborganizations. The project team (PT) 62704-1 is led by Dr. Andreas Christ, who kindly agreed on sharing the latest version of the draft as material for this chapter. The full name of the standard is "Recommended Practice for Determining the Peak Spatial-Average Specific Absorption Rate (SAR) in the Human Body from Wireless Communications Devices, 30 MHz – 6 GHz - Part 1: General Requirements for using the Finite Difference Time Domain (FDTD) Method for SAR Calculations". [35]

This standard defines the methodology for the application of the FDTD method. The scope includes e.g. the validation of numerical models of devices, uncertainty in SAR

simulations, procedures to determine the peak spatial-averaged SAR (psSAR) in a cubical volume and the correct implementation of the FDTD simulation software. This standard is applied in the SEMCAD program introduced in the next subschapter, especially in the post processing with the SAR distribution algorithms used to calculate the actual results of this thesis. [32]

The definition for SAR calculation in short states that since the electric fields in the FDTD grid (or mesh) are located on the voxel edges, all 12 of those components shall be linearly interpolated and summed to define the power dissipation at the voxel center, for which the tissue density and conductivity are unambiguously specified, even if the voxel is located at interfaces of different materials. The SAR averaging specifications of the RF exposure standards (mentioned earlier in Chapter 2.2) shall be respected and the averaging software shall provide means to comply with those definitions, for example the possibility to choose extremity tissues and body regions according to the exposure standard. [35]

This FDTD standard then gives definition for choosing the averaging cubes among the voxels in different parts of the grid, especially near and in the outer voxels. The orientations of the cubes used for SAR averaging shall align with the coordinate axes. The cubes that have at most 10 % of background material (i.e. space) and no faces completely in background material, are called valid cubes and their center voxel is assigned with the averaged SAR value. Also the voxels that have not been the center of, but fully a part of a valid cube, will be assigned with the largest SAR of the possible cubes. [35]

The voxels that have partially been part of a valid cube, will have a new cube constructed with that voxel centered on one of the six faces of the new cube. The other five faces will then grow evenly and the SAR will be the largest averaged value found amongst the smallest 5 % of possible cubes achieved this way, regardless of how much background they enclose. If the required mass for the averaging cube is not achieved, a ratio of the total power dissipated in the tissues of the entire achieved mass shall be the SAR value. [35]

The growing averaging cube became an issue at the early simulations of this study, when the SAR values were calculated for pinna tissues only. In some CAD models both of the ears were in the same CAD part, from which the pinna SAR was calculated. This caused the SAR cube to have mass also from the ear in the other side of the head. Later, this was avoided by adding a special RightEar -named sensor volume around the ear closer to the phone, from which the pinna SAR could be calculated for that ear only. This phenomena appeared usually with the child models, which don’t have the required 10 g of mass in one ear. This is also one of the reasons, why we will concentrate on head only SAR values in the results section of this thesis.

3.1.3 SEMCAD X

Simulating the EM fields in a realistic human and mobile phone CAD models require a powerful and versatile environment capable of using the computational power of the hardware. EM field propagation values are solved in the computational mesh grid constructed from the given objects in the modeling space. Depending on the model parts, the final computational domain may consist of tens of millions of small cubes made in the discretizing phase before the simulation. These cubes are called voxels, but in context of FDTD simulation the individual grid parts are referred to as cells, usually with the prefix M for million, i.e. MCells. This quantity is often used to give an estimate of the computational performance by defining the speed of the simulation in MCells per second (MCells/s). Current processors alone can reach the speed of some tens of MCells/s. But with the introduction of hardware acceleration, which refers to the utilization of graphics processing unit (GPU) cores of a graphics card, the speed rises considerably. Graphics cards are available solely for this purpose and they offer computational speeds up to the magnitude of GCells/s.

Our choice of environment was the SEMCAD X software, one of the most distinguished EM field simulation tools available, made according to the demands and with the help of the scientific community. There are other programs available, but some small details make SEMCAD the best choice in this area of research. For example, after the EM simulation phase, SEMCAD offers very advanced way of choosing individual parts of the model, e.g. specific tissues for post-processing and SAR evaluations.

The main interface of SEMCAD is similar to many other CAD tools, shown in Figure 4. The settings window on the right consists of the tabs Model, EM-Simulations, Thermo-Simulations, Measurements and Viewers. The Model tab looks like a basic folder tree, where the CAD objects are listed. In both simulations tabs, simulation tasks are set according to the project demands. In this thesis, we only run the EM simulations, but also thermal simulations with the same models with some additional settings e.g. heat capacity and thermal conductivity would be available. We also do not utilize the Measurements tab, which is used for actual measurement data processing. The most interesting tab is the last one on the right, the Viewers tab, where the post-processing results and visualizations are collected.

Part of the electromagnetic simulations in this thesis were made with older versions of the software, 14.0 and 14.6, but all the post-processing and SAR calculations were made with the newest available version at the time, SEMCAD X 14.8, which applies the IEC 62704-1 requirements with the FDTD method. [32]

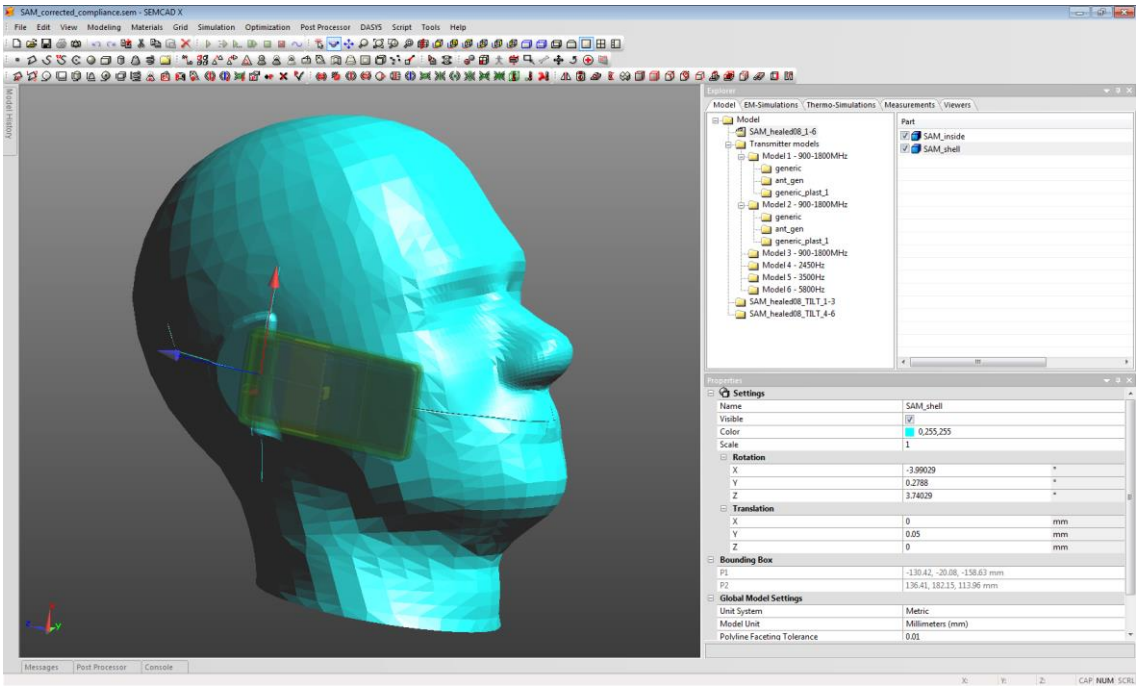

Figure 4. *SEMCAD X program main window with specific anthropomorphic mannequin (SAM) phantom and generic phone CAD models. Simulation settings window for model parts on the right.*

3.2 MRI based human head and hand models

The motivation and source of many of these models is a study conducted by the IEC 62209-1 Maintenance Team (MT1) led by Dr. Jafar Keshvari. In 2010, an interlaboratory project was initiated with the aim to assess the conservativeness of SAM phantom relative to the anatomically correct models of the human head exposed to the handheld handset models with frequencies between 800 MHz – 6 GHz.

Six different head CAD models were used (three adults and three children), exposed to five different frequencies between 900 MHz and 5.8 GHz induced by six different transmitters with varying antenna geometry and location (different frequencies require different antenna geometries matched to the wavelength i.e. only selected frequencies were used by each transmitter). This project is also referred to as SAM Phase III project for the two previous phases of SAM conservativeness studies. [36]

Inspired by the SAM conservativeness study, similar configurations and the same head models were decided to be tested in this study. The currently ongoing project of the Foundation for Research on Information Technologies in Society (IT'IS) called Virtual Population (earlier the Virtual Family (VF)) providing medical image based CAD models of different subjects provided the models of two adults (Duke and Ella) and three children (Billie, Eartha and Thelonious) for the SAM study. Additional to these, two older adult models (Visible Human male (VHM) and European Female (EF)) and two children (3-year old and 7-year old) used in different studies over the years were includ-

ed in the older Nokia simulation project and for that also added to the configurations in this thesis. This gives us the total of four adults and five children, shown in Figure 5. The eyes of the Virtual Population models have been covered for anonymity, as instructed by IT'IS. Additionally, sagittal bisections of voxelled versions of the heads can be found in Appendix D. These can be used to review the gridding and the approximate accuracy of the head tissues. [36] [41] [42]

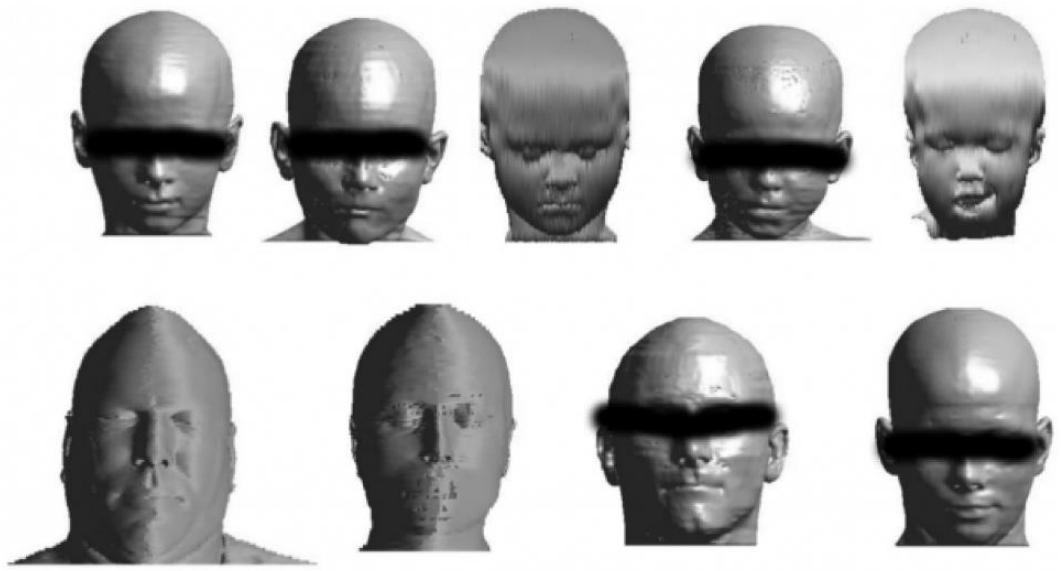

Figure 5. *Anatomical head models (from left to right) - upper row: Billie (11 years), Eartha (8 years), Brucky (7 years), Thelonious (6 years), Indy (3 years), lower row: Visible Human (38 years), HR-EF1 (40 years), Duke (34 years), Ella (26 years). All head models are displayed at the same scale. [37]*

For comparison to the real-world laboratory measurements, an accurate CAD model of the SAM phantom was also required. This is originally provided in the Amendment 1 of the standard 1528-2003 [38] and visible in the SEMCAD program in Figure 4. The properties of the CAD models have been collected to Table 3. The adults are of ages 26 to 40 and the children of 3 to 11. The heights and body mass indexes are near the average human measures, except perhaps for the earliest of these models, the Visible Human male, which is based on cryosection of an executed American prisoner, who agreed to give his body for scientific purposes. All the measures are not available in detail, but they can be estimated from the CAD models. The other models are based on magnetic resonance (MRI) imaging and partly on other types of medical imaging.

The tissues present on the model files are difficult to count precisely, since the amount of different tissues depends on the way of tissue separation in the source files. Mostly the whole body number refers to the amount of different CAD parts that can be assigned with different dielectric properties, but again with the VHM model the amount of tissues refers to the actual separated tissues from the cryosections. The head tissue counts are more precise, since they can be explicitly counted from all the CAD files. Here, the

tissue types announced by the sources of the models and the amounts of actually separated CAD parts in the simulation are both given. The head tissue part amounts are the most important numbers we need, since the models were cut from the neck up for the simulation and the differences in the EM field propagation are based on the tissue domains with different dielectric properties. [39] [40] [41] [42] [43]

Table 3. *Human models used in the simulations.*

Name	Sex	Age	Height (m)	Weight (kg)	BMI (kg/m²)	Head tissues*	Total tissues**	Origin
HR-EF1	female	40				13 / 27	15	MRI
VHM	male	38				15 / 51	100+	Cryo
Duke	male	34	1.77	72.4	23.1	27 / 50	77	MRI, VF
Ella	female	26	1.63	58.7	22.0	27 / 48	76	MRI, VF
Billie	female	11	1.47	35.4	16.5	27 / 48	75	MRI, VF
Eartha	female	8	1.36	30.7	16.7	27 / 48	75	MRI, VF
Brucky		7				12 / 33	20	MRI
Thelonius	male	6	1.17	19.3	14.0	27 / 48	76	MRI, VF
Indy		3				12 / 32	32	MRI

*) Tissue types / actual amount of separated tissues in simulation

**) Original separated tissue and organ types extracted from source

Hand models in the SAM Phase III study were chosen to represent different ways to include a hand on the simulation. Adult grips numbered 1, 2 and 4 were somewhat similar to each other, the difference being mostly in the amount of different tissues. Grips 1 and 4 are both homogeneous but the different CAD parts in Grip 4 are movable in case grip adjustments are needed. However, in this study the hand was unmodified to maintain comparability to the SAM Phase III study. The grip numbered 3 was considerably smaller, sized to belong to a child aged similarly to the head models. The grips are collected to Table 4 and shown in Figure 6. The separated tissues present in the simulated version of the grips are given on the right. The hands are cut near the lower ends of Radius and Ulna, the two major forearm bones, so despite these the tissue amounts refer to the actual hand tissues.

Table 4. *Grips from SAM Phase III project.*

Grip	Origin	Tissues in simulation
Grip 1	CTIA adult hand model	1
Grip 2	MRI based adult hand model	25
Grip 3	MRI based child hand model	18
Grip 4	The adult CAD hand model of the adult hand	9

Figure 6. *Hand models (from left to right) in the order from Grip 1 to 4. Aligned using the Nokia 8310 phone model as reference. [37]*

With these head and hand models, the simulated configurations were defined by using the adult hands with the adult heads and the child hand with the child heads, respectively. For adults this gives three times four i.e. twelve different configurations and for children five different configurations.

3.3 CAD based Nokia mobile phone models

Nokia Electromagnetic Fields (EMF) team in the old organization from 2012 consisted of the employees working on the EM safety and SAR testing issues. Part of the research side related to SAR worked closely with the IEC MT1 and therefore the group was constantly updated with the latest studies and knowledge about this scientific field. From the materials provided by Nokia, these two GSM phones were also used in the older project comparable to the project of this thesis, but without the hand models. The origin of the phones is in the beginning of 2000s, when these phones were designed for manufacturing. The basic models of the handsets are shown in Figure 7 and Figure 8.

It can be seen in the model files, that some modifications have been made to use the models especially for this kind of purpose, i.e. EM simulation. For example, in the antenna parts (which in both models are located in the upper back compartment of the casing) there has to be a feed point edge source for the EM simulation, which requires a small gap between the antenna base and the antenna element. The antenna element is designed specifically for the intended wavelength(s) so that the shape and dimensions are compatible to form the intended waveform and radiating pattern. Even though in EM simulations we use a simplified harmonic simulation mode with sinusoidal waveform, the EM field distribution is modelled correspondingly to a real device. [32]

Figure 7. *Nokia 6630. [44]*

There are both pros and cons with the selected models when considering a realistic exposure scenario. The models are admittedly old and their technology and design is different from the current mobile phones. They are thicker and more block-like and the antenna parts are more robust along with the other PEC (perfect electric conductor) parts. However, this is also a good thing. Since the simulation accuracy is our main concern and limitation, it must be noted that the more complex PEC elements would be computationally costly to model. The more accuracy is needed, the smaller grid step is required and the longer the simulation will take. Also remembering the fact, that the grid is at least in our simulations rectangular, so modeling round shapes requires even smaller grid step to avoid excessive staircasing and loss of accuracy.

Figure 8. *Nokia 8310. [45]*

Also, these models have convenient operating frequencies. These are along with other facts collected to Table 5. The uplink frequencies are the ones that the phone uses to

transmit data in the networks listed respectively. Wideband code-division multiple access (WCDMA) is the name for the air interface standard that is most used in the Universal Mobile Telecommunications System (UMTS), which is a third generation (3G) mobile cellular system for networks based on the Global System for Mobile Communications (GSM) standard. These are also the exact frequencies set for the harmonic simulations with these phone models. In Nokia 6630, the WCDMA frequency has its own feed point, since it uses two different antenna elements with their own feeds accordingly. In the lower part of the table the actual measured SAR values for the phones can be found. As we can see, they are well below the limits of 1.6 W/kg (US, 1 g averaging mass) and 2 W/kg (EU, 10 g averaging mass). The target powers in production and the measured total radiated powers provided by the original Nokia documents could be used to normalize and validate the simulated results, although in our case a more straightforward normalization to 1 W input power using the simulated feed point power as reference is used. [7] [48] [49]

Table 5. *Technical specifications of Nokia 6630 and Nokia 8310. [46] [47] [48]*

	6630 - "Charlie"	**8310**
Dimensions	110 x 60 x 21 mm (4.33 x 2.36 x 0.83 in)	97 x 43 x 19 mm (3.82 x 1.69 x 0.75 in)
Weight	127 g (4.48 oz)	84 g (2.96 oz)
SIM	Mini-SIM	Mini-SIM
Available	2004	2002
Networks	GSM tri-band (900/1800/1900) and UMTS 2100	GSM 900/1800
Uplink frequencies	GSM900 897.6 MHz, GSM1800 1747.6 MHz WCDMA 1950 MHz	GSM900 902.4 MHz GSM1800 1747.4 MHz
Connectivity	UMTS, EDGE, Bluetooth	GPRS, Infrared port
Battery	Li-Ion 900 mAh battery (BL-5C)	Li-Ion 830 mAh battery (BLB-2)
Stand-by	Up to 264 h	100 - 400 h
Talk time	Up to 3 h	2 - 4 h
SAR (US)	0.55 W/kg (head) 0.58 W/kg (body)	
SAR (EU)	0.83 W/kg (head)	0.82 W/kg (head)
Target power in production	GSM900: 32.5dBm = 1.77827941004W	GSM900: 32dBm = 1.584893W
	GSM1800/1900: 29.5dBm = 0.891250938134W	GSM1800: 29dBm = 0.7943282W
	WCDMA: 21dBm = 0.125892541179W	

Measured total radiated power (TRP) in freespace	GSM900: 28.3dBm = 0.67608W	GSM900: 28.8dBm = 0.7586W
	GSM1800: 24.6dBm = 0.288403W	GSM1800: 28dBm = 0.63096W
	WCDMA: 17.8dBm = 0.060256W	

3.4 Model modifications

The head models of SAM Phase III were all provided in pre-modified form to ensure applicability in different labs with different EM simulation software. Also, the models had their ears compressed towards the head to be on a more realistic position for cell phone usage situation. This means, that the ear is slightly compressed towards the head caused by the pressure applied by the hand holding the mobile device against the ear. The CH3, CH7, EF and VHM models from previous projects also had compressed ears. [36]

However, to avoid losing any accuracy, all the Virtual Family models were decided to be re-modified and modelled from scratch to achieve the best possible positioning and exact steps for repeatability. This required special consideration for the modeling in SEMCAD. There is a paper available about the impact of ear compression [50], which was utilized for the task. In the paper, actual physical measurements were made to assess the distance between the mobile phone and the head. A special piston device with distance and force gauges (Figure 9) was used for measurements of 28 adults and 40 children with results of 10.5 ± 2.0 mm for children (6–8 years) and 9.5 ± 2.0 mm for adults. The SAM phantom ear spacer had 10 mm distance between the device and phantom liquid in a reference measurement. The 10.5 mm distance was decided to be used for all the Virtual Family children, also for the 11 years old Billie.

The actual compression was carried out by creating a CAD model of the piston from the pinna compression paper. IEEE 1528.3 CAD model of a generic mobile phone with two intersecting cylinders was used to model the reference surface and the piston parts of the compression device. For the positioning of the generic phone, the positioning method of another paper [51] studying SAM and 14 anatomical head models was used. It will be introduced in detail in the next chapter. At this point we need to know that a reference surface through ear entrance canal points on left and right ears (EECL and EECR) and the mouth point (M) is defined and the phone positioned on the cheek position similarly to realistic laboratory measurements with the SAM phantom. After positioning the generic phone, the two cylinders were used to measure the distance for the compression by moving the other cylinder along their mutual center axis and measuring the distance between the cylinders to correspond to the distances provided by the compression paper.

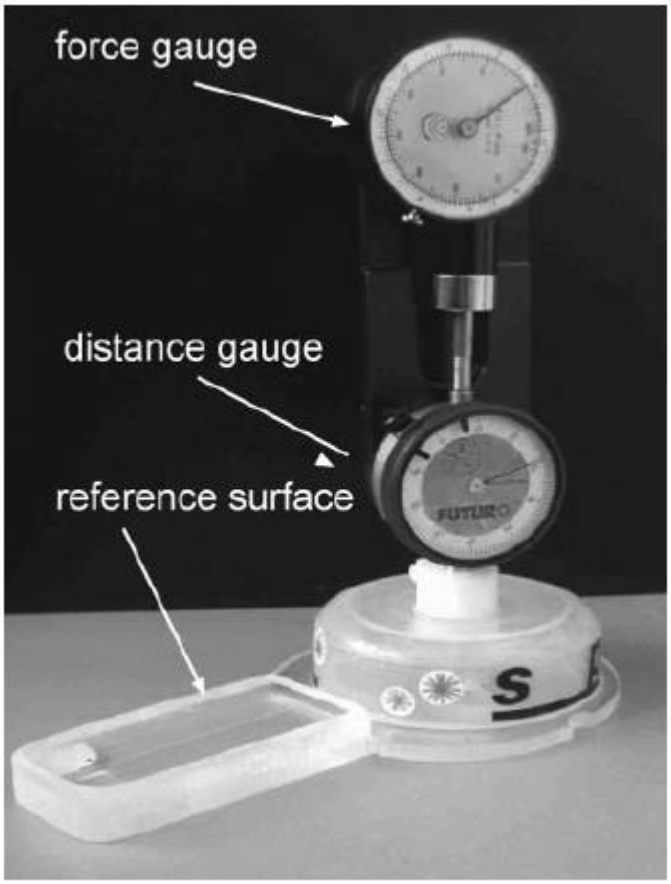

Figure 9. *Piston device used for ear compression measurements in the paper by Christ et al. [50]. Modelled CAD version was used for ear compression of the models of this study.*

Finally, the Topological Morphing Tool of the SEMCAD program (Figure 10) was used to bend the tissues i.e. ear skin and cartilage in such way that the ear approximately aligned with the distance reference cylinder surface. The thickness and dimensions of the ear were maintained by stretching the ear minimally towards the backside of the model head during the morphing process. After the morphing, the tissue masses were calculated and compared to the tissue masses of the original ear parts (Table 6). The marginal for difference was decided to be at most 5 % following the compression paper. [32] [50]

Table 6. *Ear compression mass differences as percentages of original uncompressed mass.*

	Cartilage	**Skin**	**Total**
Duke	95.75303	95.06657	**95.31036**
Ella	98.88625	103.3798	**102.4585**
Billie	96.10734	100.3618	**99.37224**
Eartha	103.8178	100.9268	**102.2825**
Thelonius	103.1325	104.2445	**103.9424**

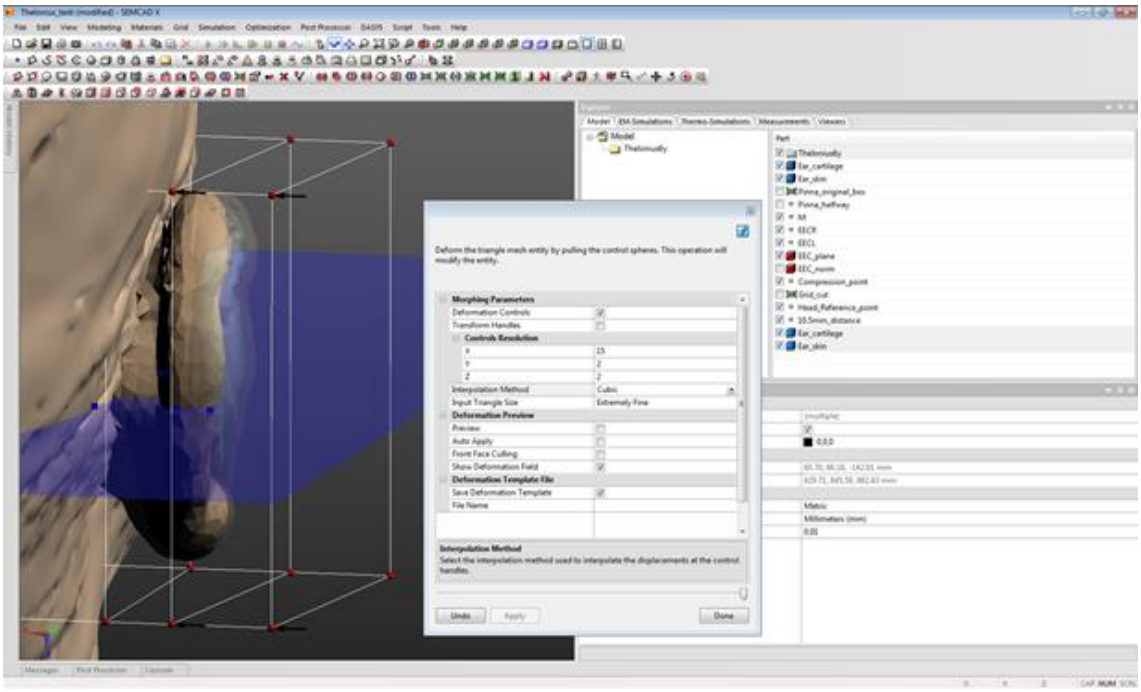

Figure 10. *SEMCAD X Morphing Tool modeling window. The EEC-M plane (blue), the compressed ear (solid skin) and the original ear (transparent shape) visible with the morphing grid (white).*

3.5 Phone positioning

The hand models in SAM Phase III were pre-configured for different handsets of the study. Conveniently, one of the handsets was a PDA-like, rather wide model similar to the 6630 and the simplified box models of higher frequencies were somewhat same size as the 8310. This made setting the grips relatively simple, starting from the top of the phone with positioning the index finger over the antenna part, which is the upper section in the back of the phone. After this the hand was rotated sideways and distance-wise around the index finger to reach as natural position for the other fingers as possible. The phone metal parts were reviewed carefully to avoid any close proximity of metal parts with the hand, since this would be a possible source for unwanted currents in the simulation. The final grips were shown earlier in Figure 6.

The hand models themselves were not modified in the process, except for the 8310 model with child Grip 3, where some modifications were needed to avoid the metallic side buttons of 8310 touching the skin voxels. Originally, parts of the middle finger were left inside the phone and touching the buttons. Air volume (light yellow in Figure 12) was added to cut the finger, because in the voxeling phase before the simulation, tissues and parts are voxelled in chosen order, which made it possible to substitute finger parts with the air. The substituted parts were only skin voxels, shown in Figure 11. There was also some overlap with the fingertips and the cheek which can be seen on the right in the second figure. At this point this was corrected by choosing the voxeling pri-

ority such that the head is voxelled after the hand, so finally the cheek skin supersedes the fingertips, leaving them in contact. Also the cut fingertip parts were only skin. However, the contact produced some very interesting results, which will be discussed in the results later.

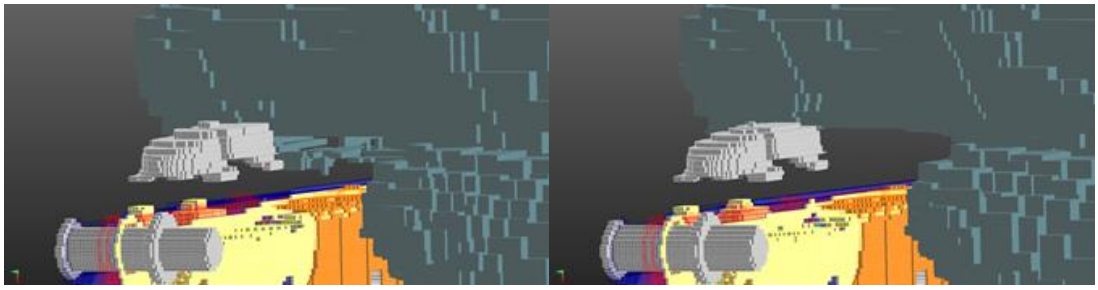

Figure 11. *Grip 3 with Nokia 8310. The skin voxels on the left were removed by an extra air volume. Final voxels on the right.*

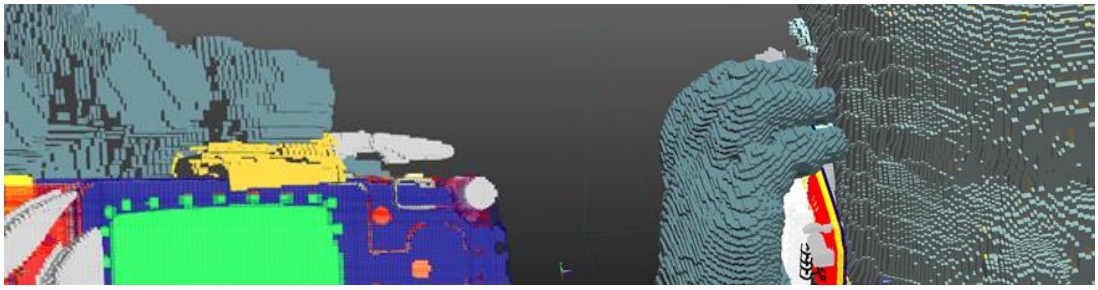

Figure 12. *Grip 3 with Nokia 8310. The extra cutting air volume (light yellow) on the left. Fingertips-cheek contact on the right.*

The hand models were positioned for the phone models in free space, but the simulation configuration requires specific location for the phone. This is based on the need for the phone to be aligned with the simulation environment coordinate axis to avoid so called staircasing issues. This refers to the process of creating a cubical grid, which is formed during the voxeling phase. The computational domain is divided to small cubes following the edges and shapes of the simulated parts along the coordinate axis to form the grid. If there are any non-orthogonal edges in the domain, the cubes form a staircase to follow the edge. This may affect the propagation of the EM fields along the computational grid in many ways, which we want to avoid.

To position the phone as precisely along the axis as possible, the phone was kept close to the origin of the axis in the simulation environment after the grip had been positioned. Only precise orthogonal rotations and unidirectional translations were applied when necessary, but usually the head model preparation phase was conducted in such way that the head in its final position was in the right coordinates to be added to the environment with the phone and the hand without further modification.

As explained before, the CH3, CH7, EF and VHM models were positioned in the earlier files of the Nokia projects and with those only the grips were added by using the phone

as a reference when adding the hand parts to the environment. Also some of the Virtual Family models were available from the SAM Phase III, but these were decided to be remodeled entirely partly because of the staircasing risk and partly to choose the grid size i.e. voxeling accuracy and the overall extent of the tissues from the original whole body models that were used to make the new heads i.e. inclusion of neck and even parts of the upper shoulders.

The standards mentioned earlier in the previous chapters, especially those related to the SAM phantom, explain the positioning of the devices in touch (cheek) and tilted position with the SAM phantom, but there is no standardization on how to position a more arbitrarily shaped realistic anatomical head model to these positions. Fortunately, Kainz et al. published a paper [51] in 2005 with a novel definition for the mobile phone positioning. This method was decided to be used to maintain possible repeatability of the study with exact operations for the process and to ensure a good comparability to the results of the other labs at the same time.

3.5.1 Positioning with anatomical heads

Because of the importance of the positioning method, it will be introduced in detail in this chapter. All the backgrounds and details can be found in the actual paper [51], but here we will point out some specific features related to SEMCAD modeling and our other settings that are based on this definition.

In Figure 13 we can see the SAM phantom reference points, which are used in describing the phone positioning with SAM. However there is a major difference between the SAM phantom ear spacer and the actual ears of anatomical head models. Natural variation of the pinna (external parts of the ear) produces an endless possibility of different configurations in the anatomical heads. Thus the reference points and planes of the SAM are too simple to be used to describe the exact location of the phone in relation to the ear and cheek.

More specifically, the line through points N (neck) and F (front), called the NF-line, plays a major role in the standards (IEEE 1528 [21] and IEC 62209-1 [25]), which define the setting of the cheek position with the following step: "*rotate the handset about the N-F line until any point on the handset is in contact with a phantom point below the pinna on the cheek*". In case of the SAM, this keeps the vertical centerline of the phone aligned with the reference plane, meaning the plane that is defined by the mouth (M) point and ear reference (ERP) points. In case of realistic anatomical models this is usually not applicable, because the NF-line over the natural pinna is rarely perpendicular to the reference plane and so the rotation described in the standards does not keep the vertical centerline of the phone aligned with the plane.

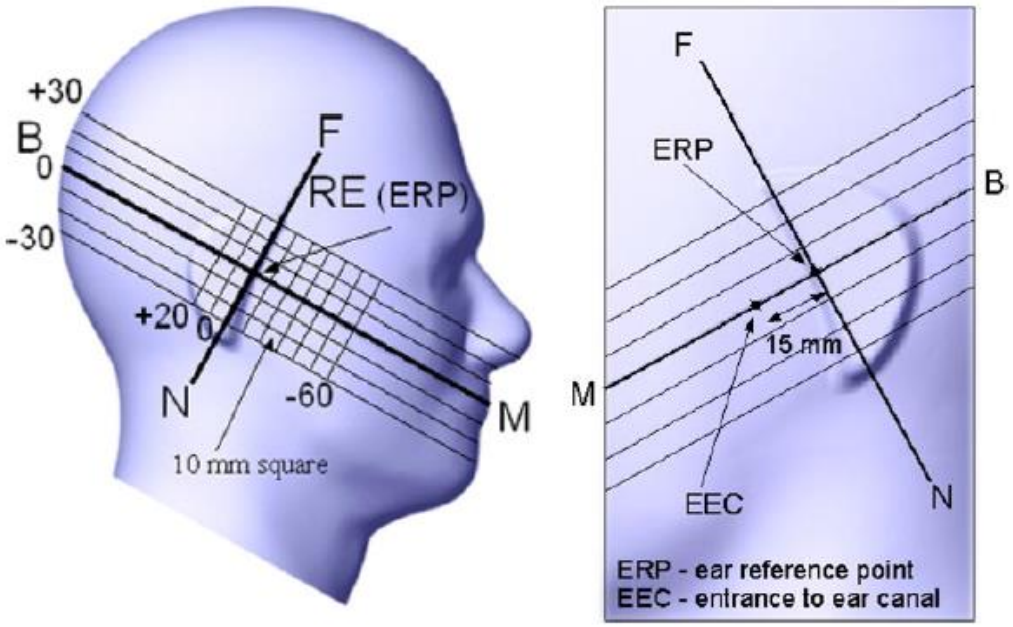

Figure 13. *SAM Phantom reference points. Mouth, Back, Neck, Front, Ear Reference Point and Ear Entrance Canal. [51] - originally in [21].*

The positioning by Kainz et al. is based on two root point sets. The overall goal is to form additional planes and lines that are specific to each head model separately, but constructed by applying the same operations using the common convention of choosing anatomical points of the head. Root point set 1 has the points we have already introduced, which are M, EECL and EECR. These are very clearly located on the mouth and ear entrances. Together they form the reference plane comparable to that of the SAM phantom. Note, that in case of the SAM the definition is with the ERP points, but with the anatomical models it is with the EEC points. The location of EEC is also shown with the SAM phantom in (Figure). Before the second set, we need distance for the Pivot Plane (DPP), which is calculated from the root point set 1 points with Equation (3.1).

$$DPP = 15\ mm \left\{ \frac{|EECL - M| + |EECR - M|}{2 * 145.5\ mm} \right\} \qquad \textbf{(3.1)}$$

DPP is the distance between ERP and EEC, which is 15 mm on the SAM phantom, scaled to the anatomical head model. This is done by comparing the distances between M and EECL/R of the anatomical model to the same measure on the SAM phantom, 145.5 mm. With this result, we can define the pivot plane to the distance DPP backwards from the line between the two EEC points (EEC-line) along the reference plane, parallel to the EEC-line and perpendicular to the reference plane. The planes are more easily understood from Figure 14 from the original paper. The DPP distances for Virtual Family models are provided in Table 7.

Table 7. *DPP calculation values for the Virtual Family models.*

Duke		**Ella**	
| EECL-M |	135.61	| EECL-M |	126.135
| EECR-M |	138.975	| EECR-M |	126.515
DPP	**14.154**	**DPP**	**13.0232**
Billie		**Eartha**	
| EECL-M |	117.716	| EECL-M |	120.417
| EECR-M |	118.046	| EECR-M |	119.805
DPP	**12.1527**	**DPP**	**12.3826**
Thelonius			
| EECL-M |	104.743		
| EECR-M |	104.47		
DPP	**10.784**		

With the pivot plane we are now able to define the neck-front (NF) line for the anatomical head. The pivot plane slices a cross section through the pinna, with a curly borderline that has a profile resembling a peeled banana. The N and F points are chosen as the boundary points of a line touching the cross section area. This is the NF-line illustrated with the orange color in Figure 14. Usually these are not the most outer points of the whole pinna (including the parts in front and back of the pivot plane), so in the final configuration with the phone, small intersections between the phone and the pinna may occur. However, after the compressing process of the pinna, the ear has a little flatter shape than initially and the intersections that occurred were insignificant.

The remaining reference planes in the figure are defined by moving the original reference plane up and down by 0.5 times the phone width. That is, the phone fits exactly between the RPU and RPD planes. Finally, the second root point set is defined by the points N and F with the last remaining addition, the tangent point T. To find that we need to draw a tangent plane (TP) through the NF-line and using the line as rotating axis, the plane is rotated towards the cheek to find the first intersecting point on the cheek between the RPU and RPD planes. That is the point where the phone first touches the cheek skin, hence called the tangent point.

As mentioned earlier, the difference in positioning the phones with anatomical head models in comparison to the SAM phantom is the choice of the reference point. For the SAM phantom the point is ERP, but for the anatomical models it is EEC. The EEC point lies on the vertical centerline of the phone, in the distance of DPP from the horizontal line defined by the standards as the perpendicular line containing the acoustic output of the handset. The cross formed by these lines is equivalent to the tangent plane. Finally, the line between the EEC points of the head model crosses the tangent plane

through the EEC reference point, which is now defined on both the phone and the head model.

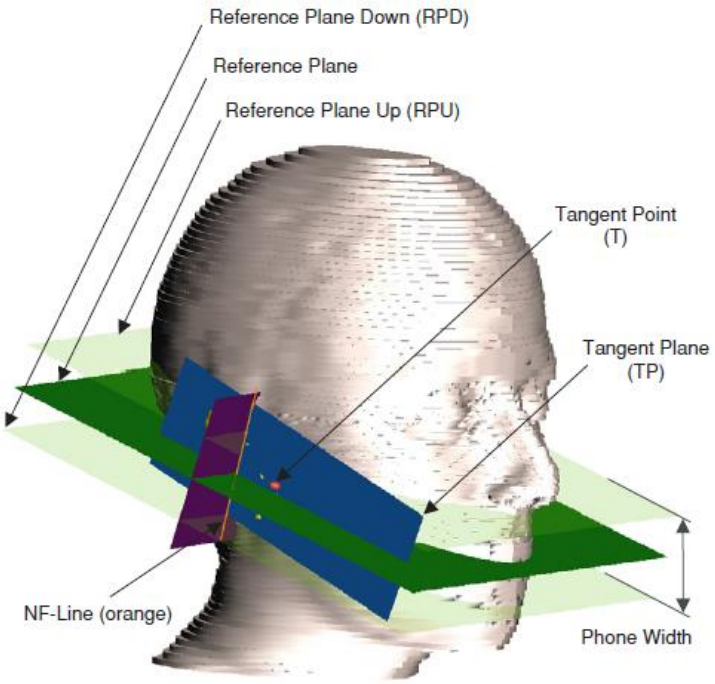

Figure 14. *Reference points of an anatomical head model by Kainz et al.[51] NF-line (orange), Reference planes (M-EEC, RPU (up) and RPD (down), Pivot Plane (purple), Tangent point (T) and Tangent plane (TP).*

With the root point sets and the reference planes, we can now find the touch and tilt positions. First, the head models were rotated to align the tangent plane with the coordinate axes. This means that the phone that is already aligned with the axes can be locked in place and only the head model with the reference points is translated to match the phone on the correct place. This is now the standardized touch position for the anatomical head. The tilt position is then obtained by moving the phone outwards along the reference line (in anatomical model the EEC-line) and then rotating the phone around the horizontal line by 15 degrees, which in our case was made by turning the head model 15 degrees, remembering that our models were aligned with the coordinate axis in touch position. The phone would then be moved backwards along the reference line until a contact with the pinna is made. In our case, the head was moved with the phone EEC reference point remaining on the EEC-line, thus achieving the same result but keeping the phone locked in place with the coordinate axis. For documentation, the distances between the EEC reference points in touch and tilt positions were collected in Table 8. The variation between 3.2 and 5.4 mm can be explained by the small anatomical differences in the pinna region, causing some phone-head combinations to intersect earlier.

Table 8. *EECref differences (along the EEC-line) between Touch and Tilt positions of the Virtual Family models.*

Duke			**Ella**		
6630	4.500	mm	6630	3.690	mm
8310	4.117	mm	8310	4.100	mm
Billie			**Eartha**		
6630	5.400	mm	6630	3.500	mm
8310	5.051	mm	8310	3.200	mm
Thelonius					
6630	3.901	mm			
8310	4.401	mm			

3.6 Simulation settings and requirements

Now that we have acquired, modified and positioned the CAD models we want to use in the simulations, we still need the settings and values to enter for the FDTD solver. Separate SEMCAD files were made for all the different configurations with single head and one of the hands for both of the phone models. For each file, the simulations were then set for different frequencies according to the uplink frequencies in Table 5.

In the simulation settings tab of the program, the harmonic simulation is chosen and the frequency given to be the main component of the excitation with the sinusoidal waveform. The program automatically calculates the corresponding wavelength, which helps both the user and the program to consider the required accuracy of the grid used for the voxeling and finally in the numerical operations, where the grid size also determines the simulation time step and thus effectively the simulation time. Even more importantly, the grid must fulfill the rule of thumb that there are at least ten cells per wavelength, which means that with for example 897.6 MHz, a minimum grid step would be 33 mm, so we naturally used much smaller step to achieve an accurate representation of the model parts. For the phone parts the smallest grid step needed was in range of a few hundred nanometers. [32]

The actual simulation duration or total time was set to be high, usually 200 periods of signal, since SEMCAD X supports automatic simulation termination, which means that during simulation, Point, Edge and Port sensors are tested for convergence, i.e. in Harmonic simulation mode steady state condition is tested. Steady state means in short explanation that the input harmonic signal has reached a constant form and is not changing over time. The threshold of the condition can be adjusted when more accurate results are needed. This usually lengthens the simulation time since the steady state is more difficult to reach.

Steady state sensor was placed in the middle of EECR-EECL (Entrance to Ear Canal Right & Left) line of the head models. The simulation auto-termination was enabled, triggered by the steady state sensor with Strict accuracy. Medium accuracy was used in some individual cases, when the simulation time seemed to be too long with the Strict setting. Basic FDTD solver was used with the axWare hardware acceleration, which enables the simulation domain to be stored in the graphics card memory and computed using the GPU in addition to the CPU calculations.

Without the acceleration, the basic FDTD solver revealed a concerning character. It found the steady state very fast and produced somewhat lower SAR results in comparison to the accelerated results. Dr. Christ suspected that there might be differences in the implementation of the absorbing boundary conditions between the solvers. Boundaries are used as the farthest sides of the FDTD domain to map the domain to infinity. For one of the SEMCADs used (there were in total 3 different versions running parallel in 3 different computers) with the basic solver, the simulation period amounts were chosen by hand according to the similar simulations completed with the accelerated solver on other SEMCAD.

To explain the concept of grid settings a little further, SEMCAD provides two gridder engines, interactive and conventional. The interactive gridder is a more automated newer version that can be used when the whole model is constructed with similar accuracy requirements. In our simulations we had the phone that needed smaller grid step in comparison to the human tissues. So more often, the conventional grid engine was used, because it gives the grid step options differently for the sensors defined for the model in the end of the modeling phase.

The sensor volumes were defined at least for the head, the hand and the phone. There was also a smaller volume added in the cheek region next to the phone, which was used to set a smaller grid step for the volume, where the highest SAR usually appears. This was set to steps under millimeter, whereas the rest of the head i.e. the whole head sensor, allowed grid steps over millimeter for the further parts of the head. At some point, a separate sensor was also added for the right ear region, for reasons related to the SAR averaging algorithm explained in Chapter 3.1.2. The sensors are used during the simulation for monitoring (like the Steady State Sensor) or to save the actual EM field values the solver produces. Both the electric (**E**) and magnetic (**H**) field values can be saved, but for SAR evaluation purposes only the E-field is sufficient, as we can see in Equations (2.7)-(2.9).

The final knowledge we need to tell the solver, are the properties of different solid regions. In case they are metal, they are set as perfect electric conductors (PEC). If they are lossy i.e. plastic or tissue, their dielectric values are given to the program. For the phones, the dielectric values for the plastic parts of different kinds of plastic were already set in the older files with the phone models and they were left as they were. Gen-

erally, the plastic is very poor conductor and thus has minor effect on the EM field. More care was given to the selection of phantom and tissue dielectric values. Firstly, the values acquired for the reference simulations with the SAM phantom are shown in Table 9.

Table 9. *SAM phantom dielectric values. Italic values are from IEEE 1528 [21].*

Frequency f **(MHz)**	**Relative permittivity** ε_r	**Conductivity** σ **(S/m)**
835	*41.5*	*0.9*
897.6	41.5	0.967415
900	*41.5*	*0.97*
902.4	41.49564	0.971004
1450	*40.5*	*1.2*
1747.4	40.07514	1.369943
1747.6	40.07486	1.370057
1800	*40*	*1.4*
1950	40	1.4
2000	*40*	*1.4*
SAM_shell	3.7	0.0016

Values were derived by calculation from IEEE 1528-2003 and SAM Extension Study project protocol of ICES TC34 SC2 WG2 by using Equation (3.2). Both conductivity and relative permittivity are obtained by extrapolating the values over the *range* of the standardized values. *Target* value is achieved by adding extrapolated value to the previous lower standardized value (*stdlow)*. [21] [52]

$$x_{target} = x_{stdlow} + (f_{target} - f_{stdlow}) \frac{\Delta x_{range}}{\Delta f_{range}} \qquad \textbf{(3.2)}$$

The dielectric values for different tissues were chosen according to the frequency, using the database provided by IT'IS [53]. These are also available as a tissue database file for SEMCAD X, which on the other hand helped the assignment in the simulation preparation phase and on the other hand eliminated the possibility for typos when the values were assigned automatically and not by hand. Only minor adjustments to the tissue names of especially the older models had to be made to ensure the correct assignments, since the tissues in the database were in certain form which differed in some of the used CAD models.

In the older Nokia project files without hand, the tissue values were from an older database and had minor differences. These values were left unchanged also in the new simu-

lations of VHM, EF, CH3 and CH7 to ensure comparability of the results between the old and new simulated configurations. All the Virtual Family simulations were made with the IT'IS database values. Generally, the differences in the values were minor and should have very little effect on the SAR results.

However, the older simulations (also referred to as REF results in the tables of Appendix A) of VHM, EF, CH3 and CH7 models have 900 MHz dielectric values also in 1747 MHz and 1950 MHz simulations. The difference in the dielectric values is only a few percent decrease in permittivity but up to 100 % increase in conductivity depending on the tissue. There was no clear explanation on this and it may cause some REF results of these cases to be inaccurate.

There are some estimates on the effect of this, for example in paper by N. Kuster et al. [54], where absorption mechanism of the energy from dipole antennas to biological bodies is discussed. According to the worst case scenario, the SAR increase with wrong dielectric values might be up to 30-40 %. Another paper by J. Keshvari et al. [55] studied the variation of dielectric values and suggests SAR differences under 20 % in 900 MHz and 1800 MHz frequencies but for smaller difference in conductivity. Also a test was made in 1747 MHz frequency with VHM and Grip 2 where the 1 g SAR increased 13 % and 10 g SAR 8 % when the dielectric values were changed from 900 MHz to 1747 MHz values.

The dielectric parameters for hands were also from the IT'IS database, except for the homogeneous hand models, where values provided in the SAM Phase III project protocol were used. These are collected to Table 10. For GSM900 and GSM1800 frequencies the values were given in the project protocol and for 1950 MHz the values were extrapolated in a similar manner as the SAM phantom dielectric values with Equation (3.2). [36]

Table 10. *Dielectric values of homogeneous hand model parts.*

Frequency f **(MHz)**	**Relative permittivity** ε_r	**Conductivity** σ **(S/m)**
897.6	30.00	0.62
902.4	30.00	0.62
1747.4	27.00	0.99
1747.6	27.00	0.99
1950	26.60	1.07

3.7 Numerical simulations and SAR averaging

After all the settings have been set, the model is voxelled and the voxels reviewed to be sure that especially the fine small structures, such as the antenna parts, have been modelled adequately. The simulations without a hand usually had 25-50 millions of cells (MCells) and the ones with a grip around 35-70 MCells. The biggest simulations were up to 80 MCells, which was in the limits considering the hardware used. Depending on the steady state, the simulations ran at minimum 20-30 periods, sometimes over a hundred. One such simulation may take time between 6 hours to over a day, so even with three computers the simulations alone took at least 6 months straight running time, considering that part of the simulations were run two or three times resulting in over 400 total simulations.

Additional to this, all the post-processing took a few hours per simulation, running on only two computers at best, for we decided to use only the newest 14.8 version of SEMCAD, which has the SAR distribution algorithm fully compatible with the IEEE/IEC 62704-1 standard explained in Chapter 3.1.2. To be more exact, the SAR values were extracted from the whole head sensor and later also additionally from the right ear sensor, averaging mass being 1 g and 10 g (remembering that US and EU SAR limits are defined for these masses) and extracting the SAR separately for all the head tissues and for head tissues excluding the ear skin and cartilage i.e. the whole ear part. This latter extraction is more comparable to the SAM phantom results, since the SAM does only have an ear spacer, and the actual E-field values can only be obtained inside the SAM liquid container and not in the ear region. It has been noted that "*SAR in the pinna can be up to 2.1 times greater than the peak spatial SAR in SAM. Measurements in small structures, such as the pinna, will significantly increase the uncertainty; therefore SAM was designed for SAR assessment in the head only.*" [51]

In settings for the SAR extraction, a few details also have to be given for the processor. The averaging algorithm can be chosen between Fast and Distribution. The Fast algorithm makes some shortcuts and does not provide full results (the difference can be seen in Figure 18 and Figure 20), which is why the Distribution algorithm was used, even though it takes sometimes much longer time. Also, the extracted frequency is chosen, here with the harmonic simulation it was obviously the only simulated frequency. For the result value, a normalization coefficient can be given, but at this point this option was not applied, since it was more practical to consider the normalization later in the analysis. At this point also the antenna mismatch can be chosen to be included, which means that if the source is not well matched, part of the input power will be reflected and less power will reach the antenna and radiate. This was also omitted at this point and thus the extracted SAR value remained as raw as possible.

Later in the analysis phase, SAR values were normalized to 1 W input power by dividing the simulated SAR values by the source feed power of the simulation. Also other

normalization would be available, since we know the real power values in Table 5. However, normalization to 1 W input power is used in other SAR studies, so it was a convenient choice. This also means that the absolute SAR values in the charts of the next chapter are not comparable to real exposure measurement scenarios but can only be used to compare the values inside a group of results obtained with this or similar simulation method.

4. RESULTS

The results were extracted from the SEMCAD post processor originally by hand. This was exhaustive and time-consuming, not to mention the obvious possibility to copy-paste and other human errors. Towards the later stages of the project, more sophisticated methods were applied, using the SEMCAD's built-in python engine, which can be used to script automated tasks for the post processor. From this point on, all the results were computed and then collected to separate text files, from which they could be combined as Excel sheets for plotting. [32]

In the Excel, the results were grouped according to desired categories, usually with one phone and head as a group. The results were normalized to 1 W input power and then compared to the corresponding simulations with the SAM phantom, which gives the result percentage for the SAM conservativeness evaluation and also normalizes the results between frequencies so that the other features in the results stand out better.

In this chapter we will see the different stages of the results and the reasons that resulted into reruns of different simulations. The preliminary results including all the results have in total 10 charts, which are provided as an appendix. Also the final results with 4 more charts with all values can be found in another appendix. The charts provided along the text have been chosen to represent all the studied questions at the same time, and thus they only have a selected collection of results in each of them.

4.1 Preliminary results

The first round including all the results from all the simulations is referred to as preliminary results in this thesis. This means 26 different phone/head/hand combinations with 5 different frequency/phone possibilities and in Touch and Tilt positions. For all of these simulations, 1 g and 10 g values for Head Only and All Tissues results were calculated, resulting in a total of 1040 values. These can be found categorized according to phone/frequency/position combination in Appendix A. One of these ten charts is shown in Figure 15 to introduce the features available in them.

In the chart there are 26 groups of columns, one for each of the head-hand combinations. The group named REF means the configuration without the hand. For Visible Human, European Female and children 3 years and 7 years old the results are from the older project for the Nokia 6630 and 8310 realistic phone models. The four results in one column are in the following order: 1 g Head Only, 10 g Head Only, 1 g All Tissues and 10 g All Tissues.

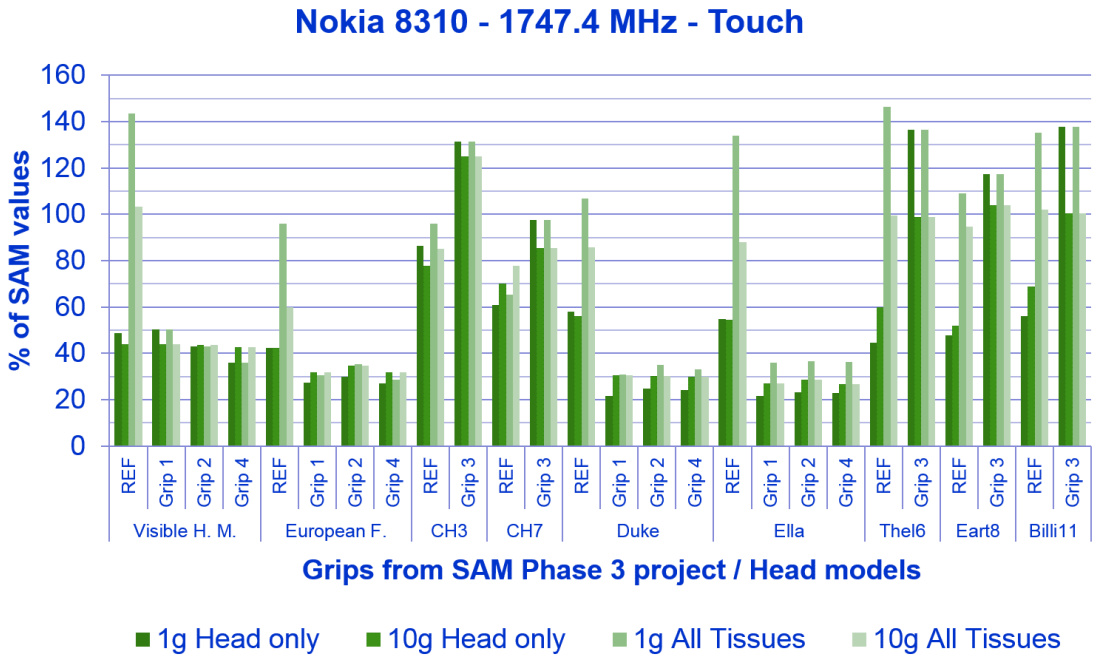

Figure 15. *Results table layout of one phone/frequency/position combination.*

For example in six different REF results in the example figure, it can be seen that the All Tissues results have significantly higher peaks. Since the only difference to the Head Only values are the ear tissues, skin and cartilage, it is clear that the SAR value peaks in the ear. This happens especially for the 1 g averaged SAR, remembering that the smaller ears don't even have a mass of 10 g, but still the ear tissues are clearly included also in the 10 g mass with the highest SAR. The Head Only SAR is, like explained before, also more comparable to the SAM phantom results and for these two reasons the boxplots later in this chapter consist of only the 1 g Head Only values. It would also generally seem at least in this chart, that the 1 g SAR is usually higher. This seems reasonable, since 1 g mass in high SAR area only has the high values in it, but the 10 g mass is more likely to include also lower SAR areas.

Considering the questions we have decided to study, we can see interesting things in the example chart. For adults, it seems that the hand (Grip 1-4) lowers the SAR values and they are in general under 60 % of the SAM phantom reference. But the children show very opposite results, indicating that the hand enhances the SAR over the 100 % SAM values, meaning that the conservativeness is not ensured. There were many other cases with equally suspicious results that can be seen in the preliminary charts.

4.2 Metal coated buttons of Nokia 8310

Some of the simulations were sent to Dr. Christ for a closer analysis, to determine what causes the enhancement effects seen in the preliminary results. A SAR hot spot was found in the middle front of the phone, meaning that the EM field was concentrated on

that area. A closer look at the material parameters revealed, that the Nokia 8310 navigation buttons, which have a chrome plating (shown in Figure 8), were set to be PEC in the simulation.

The voxel model of the phone parts with the navigation buttons in question located in the middle with the gray color can be seen in Figure 16. This material assignment seemed to be a possibly crucial contributor to the EM field formation in that area, so the material was changed to plastic for a test run. The SAR hot spot disappeared and when more tests were run, they all showed the same effect. At this point all the simulations of Nokia 8310 were decided to be rerun with the buttons set to be plastic, including also the chrome-plated side buttons which were assigned similarly as PEC in the original simulations. This meant in total 40 % of all the simulations of the project to be rerun.

The reruns produced the values collected in the charts of Appendix B. We now refer to these results as final, since the evaluations were decided to be based on the plastic button results. Both the PEC and plastic values can be compared side by side in the charts of the final results in Chapter 4.5.

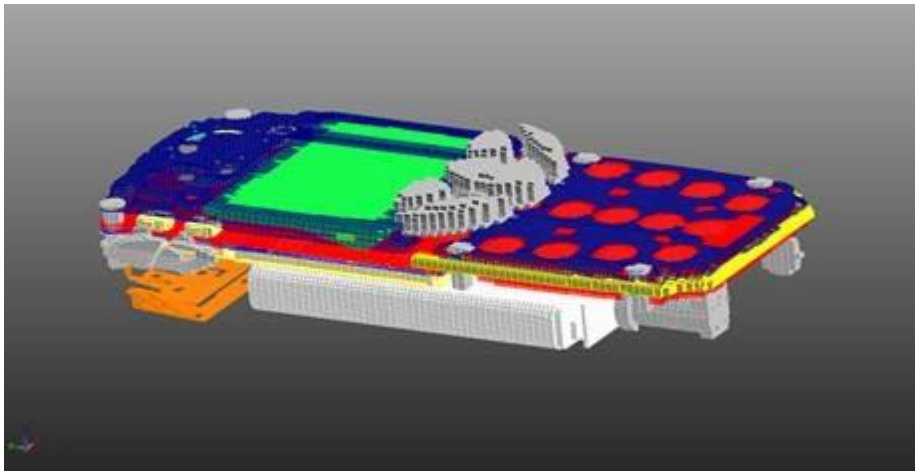

Figure 16. *PEC voxels of Nokia 8310. Antenna parts (orange) on the left and the navigation buttons (gray) in the middle.*

4.3 Child model finger-cheek contact

With the navigation buttons corrected to plastic, the general level of the SAR values showed a small drop in the touch position values. However, the child Grip 3 values still seemed to be unusually high. The higher peaks in the original values, for example those in Figure 15 dropped generally under 10 %. All the Grip 3 simulation results have been collected to the tables in Appendix C. The effect of dielectric button correction can be seen there in the dielectric corrected values, in columns 1 g SAR and 10 g SAR. The table also has the RightEar (RE) sensor values, which we will introduce in the next chapter.

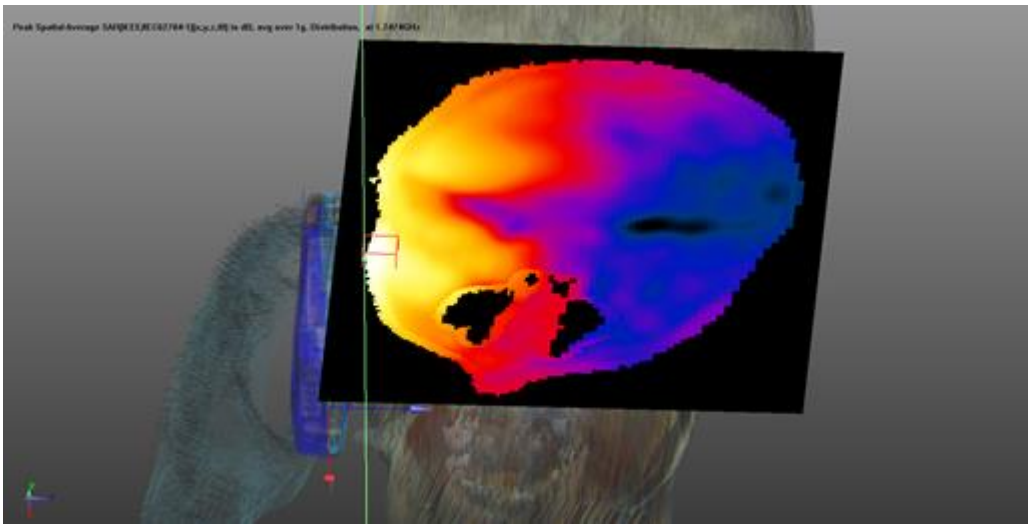

Figure 17. *Child 3yo, Grip 3, 8310 Touch, 1747.4 MHz, 1 g SAR. SAR distribution field slice. Maximum SAR in the red box volume.*

More analysis was then conducted to compare the high SAR areas of Grip 3 simulations to the other results and the slice field pictures of the SAR distributions were inspected, two of which can be seen in Figure 17 and Figure 18. It clearly seems that the simulation with otherwise the same configuration, has significantly different 1 g peak SAR location with Grip 3. In Figure 17, the slice field that has been taken from the level of the maximum 1 g cube, is on top of the 8310 phone, whereas in Figure 18, the slice and the maximum cube are clearly on lower level in the middle of the phone. We now look back to the Figure 12 and remember, how the Grip 3 was positioned with the fingers touching the cheek. It became clear at this point of the results analysis, that the connection between the fingers and the cheek has significant effect on the SAR distribution.

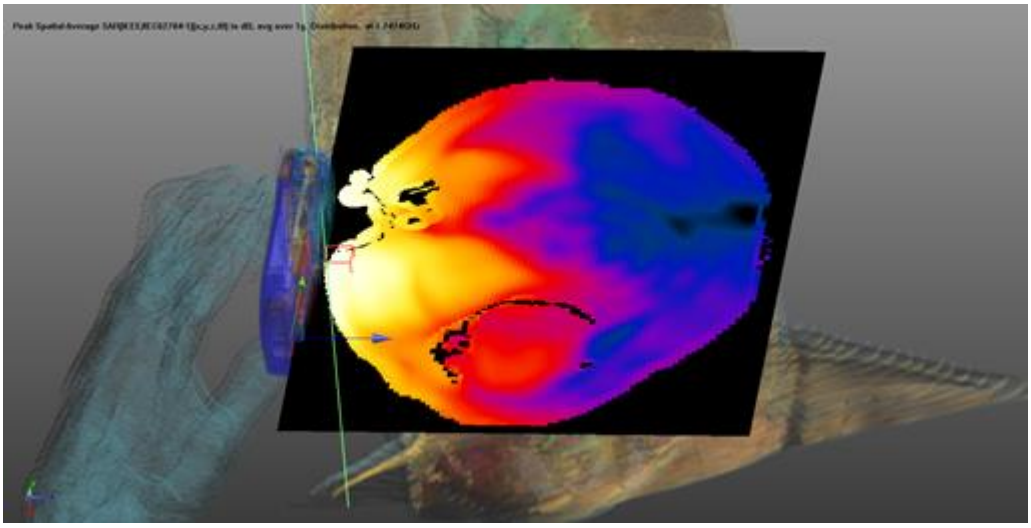

Figure 18. *Visible Human, Grip 2, 8310 Touch, 1747.4 MHz, 1 g SAR. SAR distribution field slice. Maximum SAR in the red box volume.*

This effect could also happen in the real world scenario, because tissues with sufficient conductivity in connection with each other may propagate the EM field this way. However, this is not the usual way that a mobile phone is held against the cheek and has to be considered as unnecessary enhancement of SAR. In addition, in the FDTD grid the connecting tissues are really in voxels next to each other, so the effect in calculations is as if the skin continued seamlessly from the fingers to the cheek. At this point we could almost call this an artifact of the computational results.

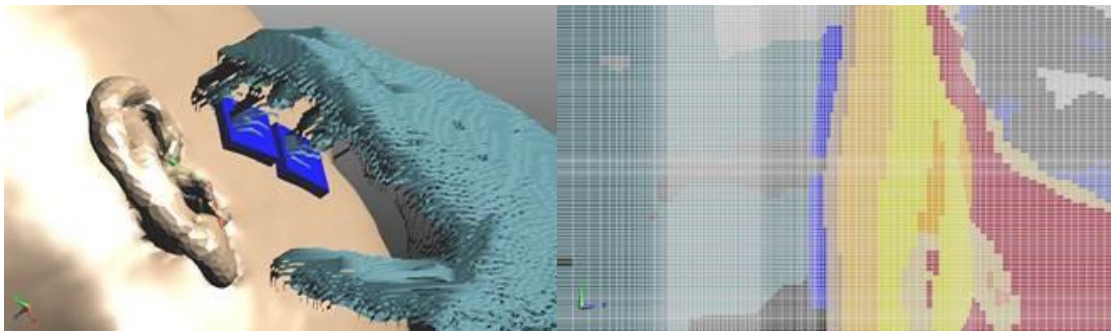

Figure 19. *Additional air blocks used to separate the fingertips from the cheek.*

It was then decided that the fingers have to be separated from the cheek, by adding small air slices between the grip and head tissues, shown in Figure 19. On the left we can see the modelled air blocks, on the right the resulting grid pictured from above, showing the blue area of air between the skin tissues. To ensure the separation in FDTD calculations, at least 2 air voxels were added everywhere, usually more. The Grip 3 simulations in touch position, with Nokia 8310, were then run for the third time. These results we add to the group of final results, substituting the uncorrected ones. The effect of the finger correction can also be seen in the tables of Appendix C. The 902 MHz values became actually a little higher, but the voxel connection effect was not clearly seen in this frequency in the first place. The 1747 MHz values however, dropped 35-65 %, which is perhaps one of the most significant results of this thesis.

4.4 Alternative E-field sensors

In the SAM Phase III project, there were separate SAR calculations for the Pinna Only SAR, meaning that only the ear skin and cartilage were included to the SAR extraction. For the reasons mentioned in Chapter 3.1.2, this required an extra sensor around the right ear area, to include only that ear in the extraction, when both ears were in the same CAD part and the ear mass was under 10 g. This sensor named RightEar was configured also in the simulation files of this project. In the reruns of the Nokia 8310 phone, also this sensor was turned on and the E-field values saved to be inspected.

A quick review of the sensors was conducted using the Fast version of the SAR averaging algorithm, which produced the slice fields in Figure 20. Firstly, we can see here the difference in the algorithm and in the illustration of the slice field, which has black area

near the sides of the slice, whereas the Distribution algorithm produces slices with the values continuing further towards the edges of the slice, visible for example in Figure 18.

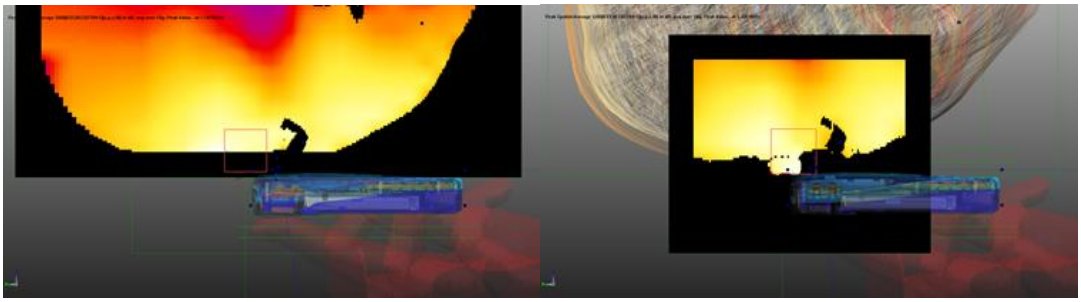

Figure 20. *E-field sensors with EF model using Fast SAR algorithm. Left: phantom. Right: RightEar.*

The slices in Figure 20 are from the same simulation with European Female. It can be seen that the 10 g cube is in the same area in both of the slices, but it is not the same. This resulted to suspicion, that the SAR values of the whole head sensor might not be the highest possible results, if the high SAR area is in the ear region, where the averaging cube is near the edge of the sensor volume.

For the remaining reruns of the 8310 model, all the RightEar sensor results were collected and the SAR values calculated for both the whole head sensor and the right ear sensor. It can be seen for example in the Grip 3 results in Appendix C, that the RightEar sensor gave different values in some simulations. For the simulations where both the sensors were available, the higher SAR value was used in the final results, to be sure that the highest possible SAR value that could be found, was used.

To explain this decision, when the RightEar sensor has a smaller value than the whole head sensor, the SAR must be in the area not completely included in the RightEar sensor. But when the RightEar sensor has a greater value, the highest SAR has to be in the ear region and not completely included in the whole head sensor. The cases where the RightEar sensor gave the higher value, were a small minority and the values were only a few percents higher. Note, that the RightEar SAR values in the finger correction table of Appendix C are compared to the dielectric results, and thus do not show the effect of the sensor.

4.5 Final results

The final results after all the corrections can be seen for Nokia 6630 in the Appendix A tables and for Nokia 8310 in the Appendix B tables. Those 10 charts present all the 1040 results in comparison to the SAM phantom. Inspecting all the results would be unpractical and exhaustive, so we now limit the following charts to the 1 g Head Only values. These are well representative and versatile to make conclusions of all the results,

since the 1 g SAR cube is likely to find the unambiguously highest SAR area of the simulated domain and the inclusion of head tissues only makes the results more comparable to the laboratory results. However it has to be remembered once more, that the presented SAR values are not absolute, but relative and meant to be compared amongst the results of this thesis only.

The plots of this chapter are called Tukey boxplots with overlaid data points. The box shows the quartiles of the data. The band inside the box is at the level of the second quartile, which is the median of the data. The top and bottom of the box are the levels of the first and third quartile. The feature that gives the name Tukey for these boxplots is the way that the whiskers are defined. Tukey's decision for the whisker length was to be 1.5 times the interquartile range (IQR) of the box, which is the difference between the first and third quartile. The whiskers are only drawn up to the points that still fall into that distance and the points that are left outside that distance are considered outliers. The plots were drawn with the RStudio program using the ggplot2 graphics library. [56] [57]

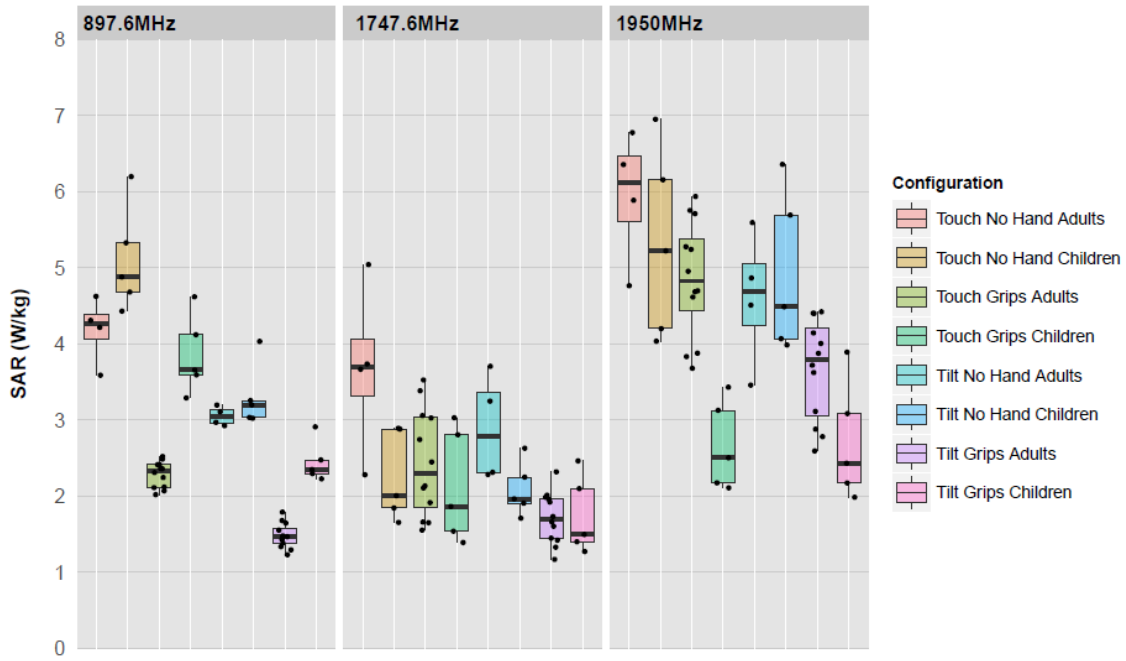

Figure 21. *Nokia 6630 SAR averaged over 1 g volume as Tukey boxplots. Touch/tilt, no hand/grips and adults/children separately. Categorized according to the frequency.*

Beginning with the 3-band Nokia 6630, the SAR results are shown in Figure 21. In 897 MHz column, it quickly stands out that every second bar is on somewhat higher level, being the simulations of the children next to the every other bar of the adults. In 1747 MHz column the differences even out and the child results seem to be even a little lower. In the 1950 MHz column the children have clearly lower values, especially the Grips values. It can also be noted that the boxplot boxes grow bigger when the frequen-

cy rises, meaning that the deviation of results grows along the frequency. The No Hand values (bars 1, 2, 5 and 6) are generally a little higher than the results with Grips, so the hand seems to generally lower the SAR. Also, the Tilt values (the last four bars of every column) seem to be lower, which is usually the case, when the phone is turned away from the head according to the tilt position definition.

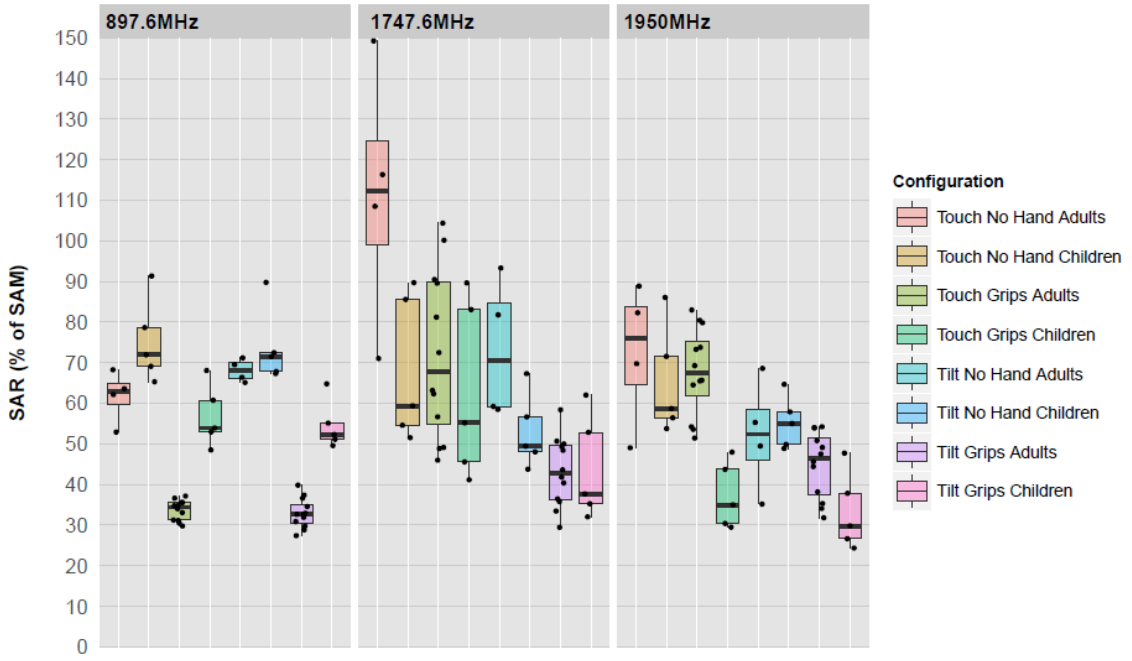

Figure 22. *Nokia 6630 SAR compared to SAM phantom averaged over 1 g volume as Tukey boxplots. Touch/tilt, no hand/grips and adults/children separately. Categorized according to the frequency.*

The values in the first chart are normalized to 1 W input power and thus they represent the simulated differences when the feed point power is taken into account. The power may change according to the matching of the antenna, which can be affected by adjacent objects, such as the hand. In real mobile phones, the device can adjust the power in these situations to keep the desired level, but in simulation the actual feed point power differences remain and affect the results, which is why we use the 1 W input power normalization. When these values are compared to the SAM results in Figure 22, the relative SAR level between the frequencies becomes more even. The comparison emphasizes the box sizes of the 1747 MHz band, showing that they have the greatest relative variation. The relative values also show that there are some results of the adults, which are over the 100 % line, meaning that the SAM phantom is not conservative in those cases.

The 1 g Head Only results of Nokia 8310 are shown in Figure 23 and Figure 24. Additional to the evaluations with the 6630, with the 8310 also the effects of the dielectric buttons and the Grip 3 finger correction can be seen. The columns with the suffix PEC are the results of the simulations with PEC navigation buttons.

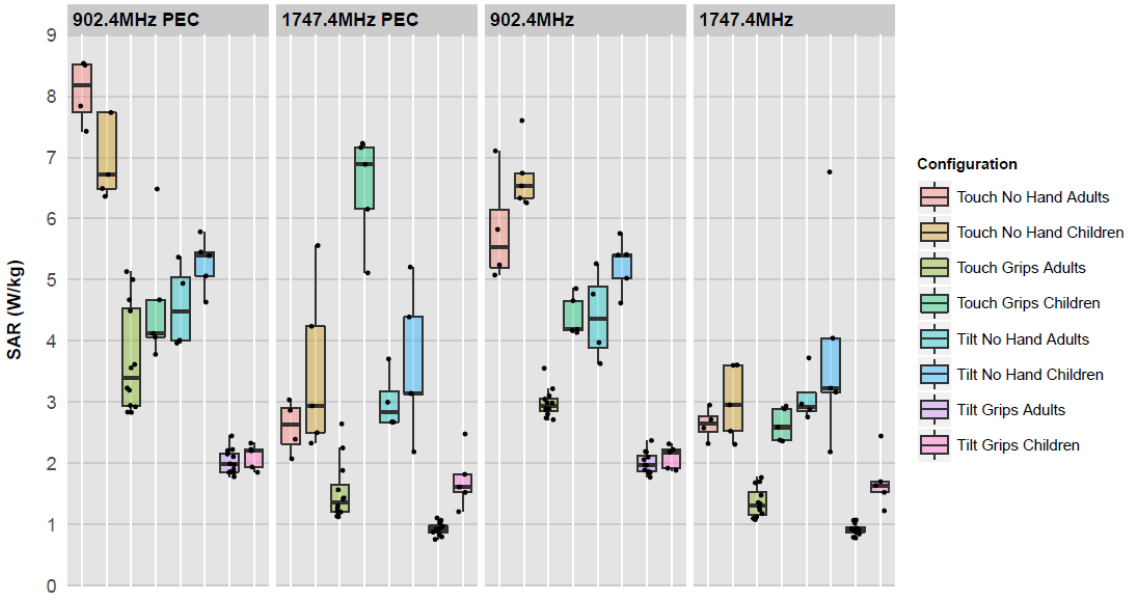

Figure 23. *Nokia 8310 SAR averaged over 1 g volume as Tukey boxplots. Touch/tilt, no hand/grips and adults/children separately. Categorized according to the frequency, results with PEC and plastic buttons separately.*

The effect of the button correction is mainly visible in the Touch results, where the SAR hot spot caused by the PEC buttons was partly inside the cheek. The corrected values for adults (bars 1 and 3) are lower but more interestingly also with less variation, especially with the grip (bar 3). The results of children (bars 2 and 4) seem to be less affected, except for the smaller variation, until we look at the difference between bar 4 in 1747 MHz PEC and dielectric button results. This is the child Grip 3 result bar and it can be clearly seen that the SAR values are on average halved after the corrections.

In the relative results with comparison to the SAM phantom, the variation amongst the 1747 MHz results is emphasized similarly as in the 6630 results. Overall, the tilt results seem to change very little after the changed button material, but there is perhaps a little tendency for the variation to get worse in the 1747 MHz results, which implies that without the SAR hot spot the EM field is differently distributed, strengthening the high areas and weakening the low areas. However, with the touch values the effect on variation is the opposite, so the field must be more even in the Touch position high SAR area.

Now concentrating on the dielectric button results, it seems that the SAR values with Grips are generally lower again. The more interesting observation can be seen comparing the values of the children and the adults. This time the children have higher SAR values in all the categories. This implies that, still after the button correction, the EM field of 8310 has higher value areas in the high conducting tissues of the heads, which are relatively larger in the juvenile heads. With Nokia 8310, the overall level of SAR remains clearly under the 100 % SAM phantom value, so for this phone the SAM seems more conservative than for the 6630.

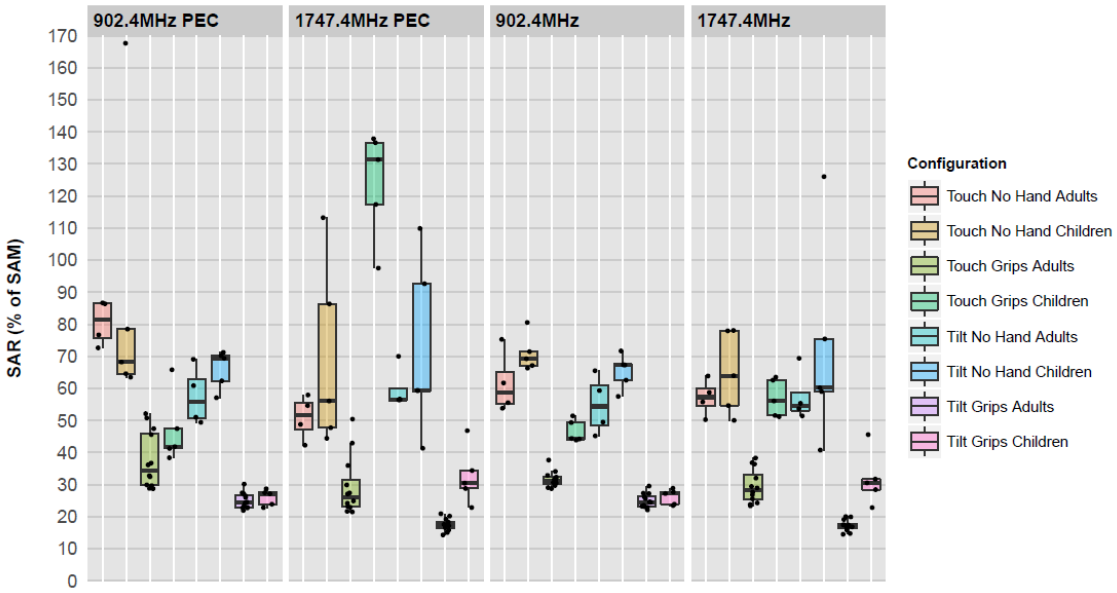

Figure 24. *Nokia 8310 SAR compared to SAM phantom averaged over 1 g volume as Tukey boxplots. Touch/tilt, no hand/grips and adults/children separately. Categorized according to the frequency, results with PEC and plastic buttons separately.*

5. CONCLUSIONS AND DISCUSSION

With the Nokia 6630 model, the children have higher values in 897 MHz frequency, but similar or lower on the higher frequencies. The lower frequency means longer wavelength and also usually deeper penetration of the field to the head tissues. Thus we can conclude that the deeper penetration combined with the smaller head size leads to relatively higher SAR values of the children in the 897 MHz frequency with Nokia 6630. For the higher frequencies, the penetration is usually smaller. There are also differences in the higher frequency results, when the grips are taken into account. The child results with the hand are clearly lower in the highest 1950 MHz frequency, but this is more likely caused by the attenuating effect of the child hand, since it can be seen in both Touch and Tilt positions.

With the Nokia 8310 model, the average level of SAR is higher for the children, both in Touch and Tilt positions, with or without the hand. The difference is somewhat clearer again in the lower 902 MHz frequency, probably caused by the different penetration depth. We know that the high SAR area for Nokia 8310 is in the cheek, so we may conclude here that the observed difference must be caused by the relatively higher amount of certain tissues in the child cheek area.

A recent paper by Foster et al. [49] collects over 20 studies that have been evaluating the RF energy absorption in child and adult models. They state that for two metrics of exposure, there is clear evidence that the age may play a factor. The SAR values will vary with the head size and hence with age in particular anatomically defined locations within the brain and in particular tissues (e.g. bone marrow) with age when the dielectric properties change age-relatedly. The second statement does not apply on this thesis, since the same dielectric values were used for all the models, which determines that the effects we have seen have to be related to the relative amounts of tissues with different conductivity values changing according to the size of the head.

The effect of the hand on the SAR results seems very clear throughout the results. All the charts indicate that the results with the grips are generally always lower than the respective results without a hand. The only clear exception to this were the simulations with the child fingers touching the face, which caused the SAR values to be almost double in comparison to the values without the tissue connection. The hand effect is based on the antenna tuning caused by the hand tissues and it varies greatly according to the antenna location of the phone model. In both Nokia devices of this thesis, the antenna is very traditionally located on the top backside of the device, so for example the

palm that might be considerable contributor to the SAR enhancement, is not near the antenna elements. [58]

Regarding the conservativeness of the SAM phantom, the 1 g and 10 g Head Only values of Nokia 6630 and Nokia 8310 have been drawn as cumulative scatter line graphs in Figure 25 and Figure 26. The All Tissues results have been omitted for the reasons discussed earlier in Chapter 3.7, we will only look at the values without the ear tissues to be as close to the conditions with the SAM phantom as possible.

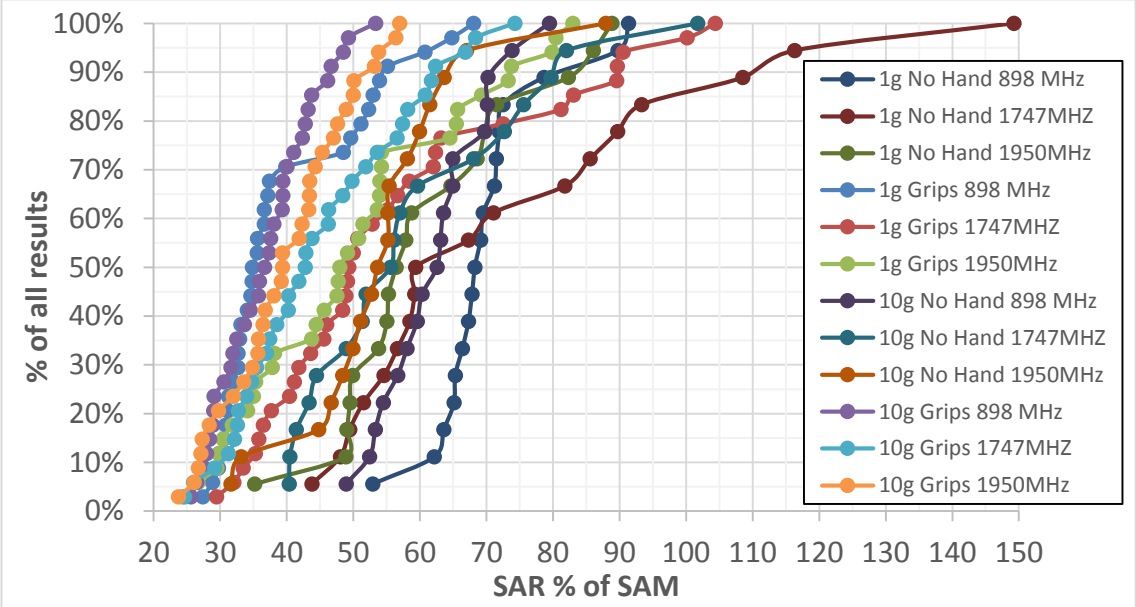

Figure 25. *Conservativeness of SAM phantom with Nokia 6630.*

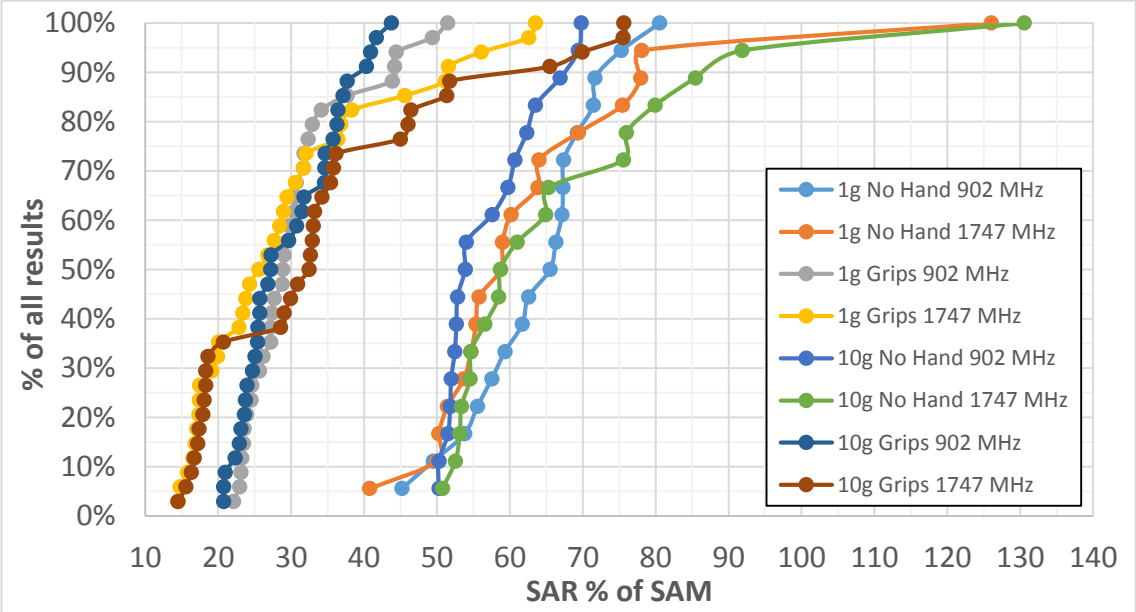

Figure 26. *Conservativeness of SAM phantom with Nokia 8310.*

SAM remains conservative with both Nokia 6630 and 8310 with the simulated head models, with and without hands. There are only a few exceptions in individual cases: With 6630 there are 6/312 cases, 1.92 %, all with Adults in 1747 MHz and with 8310 there are 2/208 cases, 0.96 %, both with CH7 1747 MHz Tilt (older model with questionable accuracy, possible second hot spot). Overall we conclude that none of the simulated configurations of this thesis gave consistently higher values than the SAM phantom. Additionally, the hand effect with Nokia 8310 can be clearly seen in Figure 26, where the four line graphs on the left are all results with the Grips.

5.1 Challenges in the numerical simulations

The standards give many indications about different possible sources of uncertainty, which have to be taken into account during the laboratory measurements. Those are generally obvious, related to electrical equipment limitations and to the somewhat unpredictable nature of EM field propagation in different materials, which still is not completely understood. All of the different technical settings of the measurements are therefore specified in the final SAR reports of the testing laboratories as instructed in the standardized testing protocols.

Also computational tasks involve various sources of possible effect on the SAR results, which are much more complex and difficult to quantify. The uncertainties and challenges observed with some of the simulation settings in this thesis are collected in the following chapters. All of them cannot be explicitly quantified but at least an estimate of the effect on SAR can be given according to the observations in different repeated simulations. Where comparable results are available, they will be given, even if they are based on individual cases.

The actual FDTD simulations are rather accurate and the repeatability is very high with exactly duplicated simulation settings, but even with the exactly same CAD models and generally agreed simulation settings, it is possible to have tens of percents difference between two research institutions. This kind of observations were made in the earlier Phase II of the SAM conservativeness evaluation work, initiated originally by ICES TC34 SC2 in 2005 to develop series of standards, IEEE 1528.1-4, to cover the numerical SAR compliance testing of personal wireless devices. This work is currently continued for example in the IEC 62209-1 maintenance team with the matters related to the presence of the hand in the simulation domain.

In comparison to the measurement results in the SAM Phase II, some results deviated more than 50 % in certain cases and multiple questions were raised about the accuracy of modeling the phone, especially the antenna elements. However, the agreement of the calculated SAR between participants was found to be similar to that of the measured SAR results in earlier studies. This shows that it is possible to obtain reproducible re-

sults, if standardized procedures and methods for numerical SAR testing can be developed. [59]

In the modeling phase of this thesis project, the modeling accuracy is based on the establishment of root point sets 1 and 2 (Chapter 3.5.1) in the beginning of the modeling. These are made by hand and thus have an accuracy limitation of a few millimeters, because the M and EEC points are not in any exact geometrical location of the realistic anatomical head models. Even though the rotations and translations as well as drawing the planes and tangents can be done with an accuracy of less than millimeter or degree, the final phone positioning might change by a millimeter or two, if the root points were set in an extremely different configuration (but still fulfilling the definition of mouth and ear entrance). Also with the tilt position setting, there is some room for error while doing the rotations and translations to achieve the tilted configuration. However, the error is still much less than what a considerably different root point set would cause.

As a reminder, the model modifications discussed in Chapter 3.4 have their own effects on the final modelled configuration, for example the choice of compressing also the ear of the 11-year old child the same amount as the 6-8 years old children and to allow 5 % mass difference in the final compressed ear generally in all the models. One of the major observations of uncertainty in this thesis related to the modeling is the effect of child Grip 3 touching the cheek skin near the high SAR and high conductivity area of the simulated configuration.

Also the material assignment of the phone parts near the head model have a similarly significant effect. These effects can be seen separately in Appendix C for both the finger contact and the PEC navigation buttons of 8310. First, the effect of navigation buttons assigned as plastic in comparison may weaken the SAR up to 30 % but also enhancement of 5 % was observed. Then the finger contact was corrected and the result compared to the plastic navigation button results, showing weakening of more than 40 % in certain cases but also enhancement of more than 10 % in others.

The old Nokia results for VHM, EF, CH3 and CH7 with 6630 and no hand, which can be seen on the Appendix A charts as the REF values and in Chapter 4 as part of the no hand boxes in the plot, are the most unreliable results presented. They were simulated with slightly looser gird meaning less voxels i.e. with less accuracy in some areas of the phone and head. However, the accuracy is not actually the issue, but the difference in the dielectric values mentioned in Chapter 3.6. The simulations were originally run with 900 MHz dielectric values for the head, which has some impact to the results. We have run a few repeated simulations with VHM and Grip 2, which show that the results with correct dielectric values are 13 % higher for 1 g SAR and 7-8 % for 10 g SAR. These results are of course affected also by the hand, so the comparison may be biased. We also have the SAM phantom simulations from both the old and new results, which can be seen in Table 11.

Table 11. *SAM phantom results in old Nokia files compared to new simulation results. SAR normalized to 1 W input power, as W/kg.*

	OLD		**DIFFERENCE**		**NEW**	
	6630		**new % of old**		**6630**	
Frequency/MHz	**SAR 1 g**	**SAR 10 g**			**SAR 1 g**	**SAR 10 g**
897.6	6.774	4.793	**100.14**	**101.30**	6.783	4.855
1747.6	3.211	2.022	**105.21**	**104.71**	3.379	2.117
1950	9.714	5.373	**73.63**	**73.84**	7.153	3.967
897.6 Tilt	4.473	3.264	**100.41**	**100.47**	4.492	3.279
1747.6 Tilt	3.906	2.307	**101.66**	**101.64**	3.971	2.344
1950 Tilt	9.833	5.447	**82.94**	**87.02**	8.156	4.740
	8310				**8310**	
Frequenzy/MHz	**SAR 1 g**	**SAR 10 g**			**SAR 1 g**	**SAR 10 g**
902.4	10.221	6.901	**96.37**	**95.66**	9.849	6.601
1747.4	4.909	2.889	**106.80**	**104.15**	5.243	3.009
902.4 Tilt	7.773	5.384	**104.45**	**105.46**	8.119	5.678
1747.4 Tilt	4.740	2.594	**111.72**	**109.90**	5.295	2.851

The effect of differences in simulation settings can be seen here; the new results are in general higher, but in the 1950 MHz simulations the effect is clearly the opposite. The old results are compared with the old SAM results and the new results with the new SAM results i.e. the plots in Chapter 4 with the SAR as percentage of SAM try to compensate the differences.

There are also minor differences and other aspects in dielectric values of the old simulations, some mentioned in Chapter 3.6 and collected in more detail to Table 12. Many of the differences are caused by the material assignment process, where some of the values have been chosen by hand and the tissue types in different models are sometimes hard to distinguish or the tissues are differently separated as CAD parts.

Table 12. *Differently assigned tissue types in old Nokia simulations.*

Tissue	**Difference**	**Effect on SAR (estimate)**
Ear skin and cartilage	Cartilage values used for both	Small (considering Head Only SAR)
Eye lens	Lens or Lens (Cortex) values alternate	Negligible
Midbrain and cerebellum	Assigned tissue type varies between frequencies	Negligible (values close to each other)
Cranial fossa and tonsils	Assigned tissue type varies between models and frequencies	Minimal

Fat, subcutaneous adipose tissue and connective tissue	Values in older files are considerably different than in current updated tissue database	Some effect on comparability between the old and new results

The effect of ear and cartilage assignment was tested by repeating one of the 6630 simulations with EF and Grip 2. The other simulation had the cartilage values on both pinna tissues and the other had the skin value corrected on the skin part. The values with the skin correctly assigned were slightly higher but the difference was not more than 1-2 % in the All Tissues SAR including the pinna, and less than 1 % in the Head Only SAR excluding the pinna.

Regarding the phone models, the CAD files from old project files were used and the simulation settings matched or sometimes tightened (smaller grid steps) to have more accuracy on the new simulations. Especially the PEC (perfect electric conductor) parts were inspected closely at the voxeling phase before the simulations. These metallic parts were modelled consistently throughout the whole project and there is very little variation in them, but with some non-PEC parts, more precisely the small plastic parts inside the phone, there were some differences between the GSM and WCDMA models of 6630. The phones were in different CAD source files having a different EM source for the antenna (because different antenna part is used according to the frequency), and for some reason the WCDMA file had a few more small non-PEC parts in comparison to the GSM file. There are in total more than a hundred non-PEC parts and their conductivity is low, so having slightly different amount of them in the area not very close to the antenna PEC parts has minimal effect on SAR results.

5.2 Future development of SAR research

The conclusions in this thesis are in line with the current trends in the SAR research. We saw some differences according to the age i.e. the head size, which seem to be related to the tissues in the cheek area. However, these results are clearly dependent on the phone model i.e. the EM field source of the simulation and its distance to the head, since the results were not the same for both of the phones, in other words not systematical. Generally, most of the differences seen in the charts were somehow related to the hand models included in the simulations.

Overall we only observed attenuation of the SAR values in the presence of the hand. A few individual and partly unrelated cases showed SAR enhancement, which is a great example showing the uncertainty and unpredictability of numerical assessment of SAR. Our results did confirm the SAM phantom conservativeness in the tested configurations, which was to some extent expected, considering that the Nokia models of this study have been tested and simulated before with conventional results.

The latest version of IEC 62209-1 includes considerations about the hand effect on the SAR values. The mechanisms of the hand effect are still not known very well, so it is likely that the future studies will take sides about including the hand in the tested configuration and they will aim to develop the understanding about the effect further. Also the methods of the computational study of SAR will continue to develop, along with more and more powerful computational capabilities of current computers. At some point, the simulations might be able to produce the SAR results as accurately as the laboratory measurements, potentially in lesser time.

After the completion of this thesis project, additional analysis has been conducted for the unusual results. Some of the deviant cases have been rerun (again) to assess the reason for their deviation. Those results will be presented in a paper prepared from the data including the results of this thesis study, which will be published soon after this thesis.

REFERENCES

[1] Official Statistics of Finland (OSF): Use of information and communications technology by individuals [WWW]. ISSN=2341-8710. Helsinki 2014, Statistics Finland. Accessed: 11.3.2015]. Available: http://www.stat.fi/til/sutivi/2014/sutivi_2014_2014-11-06_tie_001_en.html

[2] Official Statistics of Finland (OSF): Consumer survey 2012, June. Appendix figure 12. Prevalence of household appliances. Helsinki 2012, Statistics Finland. [Accessed on 1.6.2013]. Available: http://www.stat.fi/til/kbar/2012/06/kbar_2012_06_2012-06-27_kuv_012_fi.html.

[3] GSMA Intelligence. Data dashboard of Finland [WWW]. London 2015, GSMA Intelligence. [Accessed: 11.3.2015]. Available: https://gsmaintelligence.com/markets/1024/dashboard/

[4] Nyberg, H. & Jokela, K. Sähkömagneettiset kentät. Hämeenlinna 2006, Säteilyturvakeskus. 555 p. [Accessed on 1.6.2013]. Available: http://www.stuk.fi/julkaisut_maaraykset/kirjasarja/fi_FI/kirjasarja6/

[5] Young, H. D. & Freedman R. A. Sears and Zemansky's University Physics: With Modern Physics. 11th Ed. 2003, Addison Wesley. 1714 p.

[6] 3GPP TS 45.005 version 10.5.0 Release 10. Digital cellular telecommunications system (Phase 2+); Radio transmission and reception. 2012, European Telecommunications Standards Institute. 259 p. [Accessed on 1.6.2013]. Available: http://www.etsi.org/deliver/etsi_ts/145000_145099/145005/10.05.00_60/ts_145005v100500p.pdf

[7] 3GPP TSG SA #8. WARC-92 Frequencies for IMT-2000. 2000, 3GPP. 11 p. [Accessed on 1.6.2013]. Available: http://www.3gpp.org/ftp/tsg_sa/TSG_SA/TSGS_08/Docs/PDF/SP-000257.pdf

[8] Säteilyturvakeskus (STUK): Matkapuhelimet ja tukiasemat. Helsinki 2003, STUK. [Accessed on 1.6.2013]. Available: http://www.stuk.fi/julkaisut_maaraykset/fi_FI/katsaukset/_files/87327465852895286/default/katsaus_matkapuhelimet_ja_tukiasemat.pdf

[9] Finnish Communications Regulatory Authority (Ficora): Frequency allocation table. Helsinki 2015, Ficora. [Accessed on 4.3.2015]. Available: https://www.viestintavirasto.fi/attachments/maaraykset/Taajuusjakotaulukko_06022015_en.PDF

[10] American National Standards Institute (ANSI). Historical overview [WWW]. [Accessed on 24.7.2013]. Available: http://www.ansi.org/about_ansi/introduction/history.aspx?menuid=1

[11] Mason, P.A., Murphy, M. R. & Petersen, R. C. IEEE EMF Health & Safety Standards. WHO Meeting on EMF Biological Effects. Seoul 2002, WHO. Available: http://www.who.int/peh-emf/meetings/southkorea/en/

[12] IEEE C95.1-2005. IEEE Standard for Safety Levels with Respect to Human Exposure to Radio Frequency Electromagnetic Fields, 3 kHz to 300 GHz. New York 2006, The Institute of Electrical and Electronics Engineers, Inc. 238 p.

[13] Ocepchuk J.M., Petersen R.C. Historical Review of RF Exposure Standards and the International Committee on Electromagnetic Safety (ICES). Bioelectromagnetics Supplement 6:S7-S16 (2003). Available: http://grouper.ieee.org/groups/scc28/sc4/ICES%20history.pdf

[14] ANSI C95.1-1982. American National Standard Safety Levels With Respect to Human Exposure to Radio Frequency Electromagnetic Fields, 300 kHz to 100 GHz. New York 1982, The Institute of Electrical and Electronics Engineers, Inc. 24 p.

[15] IEEE C95.1-1999. IEEE Standard for Safety Levels with Respect to Human Exposure to Radio Frequency Electromagnetic Fields, 3 kHz to 300 GHz. New York 1999, The Institute of Electrical and Electronics Engineers, Inc. 73 p.

[16] International Commission on Non-Ionizing Radiation Protection (ICNIRP) 1998. Guidelines for limiting exposure to time-varying electric, magnetic and electromagnetic fields (up to 300 GHz). Health Physics 74(1998)4, pp. 494-522. [Accessed on 25.6.2013]. Available: http://www.icnirp.org/documents/emfgdl.pdf

[17] International Radiation Protection Association (IRPA). History [WWW]. [Last updated on: 1.2.2013]. [Accessed on: 25.7.2013]. Available: http://www.irpa.net/page.asp?id=10

[18] European Committee for Electrotechnical Standardization (CENELEC). Primer on Standards. Brussels 2002, CENELEC. 52 p. Available: http://oek.ove.at/CenelecInfo.pdf

[19] Sesko ry. Standardisointijärjestelmä – CENELEC [WWW]. [Accessed 1.8.2013]. Available: http://www.sesko.fi/portal/fi/standardointijarjestelma/cenelec/

[20] Institute of Electrical and Electronics Engineers (IEEE). History of IEEE [WWW]. [Accessed on: 31.7.2013]. Available: http://www.ieee.org/about/ieee_history.html

[21] IEEE 1528-2003. IEEE Recommended Practice for Determining the Peak Spatial-Average Specific Absorption Rate (SAR) in the Human Head From Wireless Communications Devices: Measurement Techniques. New York 2003, The Institute of Electrical and Electronics Engineers, Inc. 149 p.

[22] IEEE 1528-2013. IEEE Recommended Practice for Determining the Peak Spatial-Average Specific Absorption Rate (SAR) in the Human Head from Wireless Communications Devices: Measurement Techniques. New York 2013, The Institute of Electrical and Electronics Engineers, Inc. 246 p.

[23] International Electrotechnical Commission (IEC). History [WWW]. [Accessed: 9.8.2013]. Available: http://www.iec.ch/about/history/

[24] International Electrotechnical Commission (IEC). Strategic Business Plan of TC 106. Geneva 2009, IEC. Available: http://www.iec.ch/cgi-bin/getfile.pl/sbp_106.pdf?dir=sbp&format=pdf&type=&file=106.pdf

[25] IEC 62209-1 ed. 1. Human exposure to radio frequency fields from hand-held and body-mounted wireless communication devices – Human models, instrumentation, and procedures – Part 1: Procedure to determine the specific absorption rate (SAR) for hand-held devices used in close proximity to the ear (frequency range of 300 MHz to 3 GHz). Geneva 2005, International Electrotechnical Commission. 215 p.

[26] IEC 62209-2 ed. 1. Human exposure to radio frequency fields from hand-held and body-mounted wireless communication devices - Human models, instrumentation, and procedures - Part 2: Procedure to determine the specific absorption rate (SAR) for wireless communication devices used in close proximity to the human body (frequency range of 30 MHz to 6 GHz). Geneva 2010, International Electrotechnical Commission. 231 p.

[27] International Electrotechnical Commission (IEC). TC 106 Dashboard - Work Programme. Geneva 2015, IEC. Available: http://www.iec.ch/dyn/www/f?p=103:23:0::::FSP_ORG_ID,FSP_LANG_ID:1303,25

[28] Gordon, C. C., Churchill, T., Clauser, C. E., Bradtmiller, B., McConville, J. T., Tebbetts, I., and Walker, R. A., 1988 Anthropometric Survey of U.S. Army Personnel: Methods and Summary Statistics, Technical Report NATICK/TR-89/044, U.S. Army Natick Research, Development and Engineering Center, Natick, Massachusetts, Sept. 1989.

[29] EX3DV4 Smallest Isotropic E-Field Probe for Dosimetric Measurements. Probe specifications. Zurich 2012, Schmid & Partner Engineering AG. Available: http://www.speag.com/products/dasy/probes/ex3dv4-isotropic-dos-probe/

[30] DASY52 PRO Measurement system. Component specifications. Zurich 2012, Schmid & Partner Engineering AG. Available: http://www.speag.com/products/dasy/dasy-systems/dasy52-pro/

[31] Conservativeness of mobile phone SAR measurements. Mobile Manufacturers Forum Viewpoint publication. 2011. [Accessed on: 11.2.2014]. Available: http://www.mmfai.org/public/docs/eng/111025__MMF_Viewpoint_SARSAMconservativness_final.pdf

[32] SEMCAD X Reference Guide for version 14.8. Zurich 2012, Schmid & Partner Engineering AG. 465 p.

[33] Yee, K. Numerical solution of initial boundary value problems involving Maxwell's equations in isotropic media. Antennas and Propagation, IEEE Transactions on, 14(1966)3, pp. 302-307. doi: 10.1109/TAP.1966.1138693

[34] Taflove, A. & Hagnes, S. C. Computational Electrodynamics: The Finite-Difference Time-Domain Method. Michigan 1995, Artech House Inc. 599 p.

[35] IEC 62704-1 ed.1. Draft Recommended Practice for Determining the Peak Spatial-Average Specific Absorption Rate (SAR) in the Human Body from Wireless Communications Devices, 30 MHz - 6 GHz- Part 1: General Requirements for using the Finite Difference Time Domain (FDTD) Method for SAR Calculations. Geneva 2015, International Electrotechnical Commission. 79 p.

[36] SAM Conservativeness Phase III - Hand effect on SAR - Computational study aimed at verifying conservativeness of SAM phantom relative to the anatomically correct models of the human head exposed to the handheld handset models. August 2011. IEC-MT1-62209-1. Project protocol. 7p.

[37] Keshvari J., Kivento M., Christ A. & Bit-Babik G. Large Scale Study on Variation of the Realistic Exposure of Adults and Children to Cell Phones. Bio-EM2013, Thessaloniki, Greece, Jun 10 - 14, 2013. Session W2: Workshop 2: Comparison of RF absorption in heads of children and adults due to mobile phone exposures.

[38] IEEE Recommended Practice for Determining the Peak Spatial-Average Specific Absorption Rate (SAR) in the Human Head from Wireless Communications Devices: Measurement Techniques - Amendment 1: CAD File for Human Head Model (SAM Phantom)," IEEE Std 1528a-2005 (Amendment to IEEE Std 1528-

2003) , vol., no., pp.1,11, Feb. 24 2006. doi: 10.1109/IEEESTD.2006.99106. Available: http://ieeexplore.ieee.org/stamp/stamp.jsp?tp=&arnumber=1603350&isnumber=33682

[39] Andreas Christ, Nicolas Chavannes, Neviana Nikoloski, Hans-Ulrich Gerber, Katja Pokovic and Niels Kuster. A Numerical and Experimental Comparison of Human Head Phantoms for Compliance Testing of Mobile Telephone Equipment. Bioelectromagnetics 26:125-137 (2005). Zurich, Switzerland. Available: http://www.speag.com/assets/downloads/publications/Christ2005.pdf

[40] United States National Library of Medicine. Visible Human Project Fact Sheet [WWW]. [Updated 29.7.2013]. [Retrieved 25.2.2014]. Available: http://www.nlm.nih.gov/pubs/factsheets/visible_human.html

[41] Andreas Christ, Wolfgang Kainz, Eckhart G. Hahn, Katharina Honegger, Marcel Zefferer, Esra Neufeld, Wolfgang Rascher, Rolf Janka, Werner Bautz, Ji Chen, Berthold Kiefer, Peter Schmitt, Hans-Peter Hollenbach, Jianxiang Shen, Michael Oberle, Dominik Szczerba, Anthony Kam, Joshua W. Guag and Niels Kuster, The Virtual Family – Development of Surface-based Anatomical Models of Two Adults and Two Children for Dosimetric Simulations, in Physics in Medicine and Biology, Volume 55, Issue 2, pp. N23–N38, January 2010

[42] Foundation for Research on Information Technologies in Society. High-Resolution Human Models: Virtual Population [WWW]. [Retrieved: 25.2.2014]. Available: http://www.itis.ethz.ch/itis-for-health/virtual-population/human-models/

[43] Andreas Christ, Marie-Christine Gosselin, Maria Christopoulou, Sven Kuhn and Niels Kuster. Age-dependent tissue-specific exposure of cell phone users. Phys. Med. Biol. 55 (2010) 1767–1783. doi:10.1088/0031-9155/55/7/001. Zurich, Switzerland. Available: http://iopscience.iop.org/0031-9155/55/7/001/pdf/pmb10_7_001.pdf

[44] Nokia 6630 - Scheda Tecnica. Tecnozoom - La guida all'Hi Tech [WWW]. [Accessed: 1.4.2015]. Available: http://www.tecnozoom.it/cellulari/foto-nokia-6630-pag-5.html

[45] Nokia 8310 - Chi tiết sản phẩm [WWW]. [Accessed: 1.4.2015]. Available: http://dienthoaico.webmau.vn/chi-tiet/nokia-8310-3450.html

[46] Nokia 6630 - Phone and User’s Guide. Nokia Corporation. Helsinki 2004-2005. Available: http://nds1.nokia.com/phones/files/guides/Nokia_6630_UG_en.pdf

[47] Nokia 8310 - Phone and User's Guide. Nokia Corporation. Helsinki 2002-2004. Available: http://nds2.webapps.microsoft.com/files/support/apac/phones/guides/Nokia_8310_APAC_UG_EN.pdf

[48] 6630 & 8310 Simulation project – All results (Excel file). Nokia internal document. Electromagnetic Fields Team. 2011.

[49] Foster K. R., Chou C.K., Are Children More Exposed to Radio Frequency Energy From Mobile Phones Than Adults? IEEE Access vol. 2 2014. doi: 10.1109/ACCESS.2014.2380355. Available: http://ieeexplore.ieee.org/stamp/stamp.jsp?reload=true&arnumber=6982034

[50] Christ, A., Gosselin, M.-C., Kühn, S. and Kuster, N. (2010), Impact of pinna compression on the RF absorption in the heads of adult and juvenile cell phone users. Bioelectromagnetics, 31: 406–412. doi: 10.1002/bem.20575

[51] W. Kainz, A. Christ, T. Kellom, S. Seidman, N. Nikoloski, B. Beard and N. Kuster (2005). Dosimetric comparison of the specific anthropomorphic mannequin (SAM) to 14 anatomical head models using a novel definition for the mobile phone positioning. Physics in Medicine and Biology, vol. 50, no. 14, pp. 3423. doi:10.1088/0031-9155/50/14/016

[52] Protocol for the Computational Comparison of the SAM Phantom to Anatomically Correct Model of the Human Head at Extended Frequencies: 300 MHz – 5.8 GHz. IEEE ICES TC-34, SC-2, WG-2 November 29, 2006 (revised March 2, 2007).

[53] Hasgall PA, Di Gennaro F, Baumgartner C, Neufeld E, Gosselin MC, Payne D, Klingenböck A, Kuster N, "IT'IS Database for thermal and electromagnetic parameters of biological tissues," Version 2.6, January 13th, 2015. Available: http://www.itis.ethz.ch/database

[54] N. Kuster and Q. Balzano. Energy Absorption Mechanism by Biological Bodies in the Near Field of Dipole Antennas Above 300 MHz. IEEE TRANSACTIONS ON VEHICULAR TECHNOLOGY, VOL. 41, NO. 1, FEBRUARY 1992.

[55] J. Keshvari, R. Keshvari and S. Lang. The effect of increase in dielectric values on specific absorption rate (SAR) in eye and head tissues following 900, 1800 and 2450 MHz radio frequency (RF) exposure. Phys. Med. Biol. 51 (2006) 1463–1477. doi:10.1088/0031-9155/51/6/007. Available: http://iopscience.iop.org/0031-9155/51/6/007/.

[56] R function manual. ggplot2 0.9.3.1 - Box and whiskers plot [WWW]. [Retrieved 15.5.2015]. Available: http://docs.ggplot2.org/0.9.3.1/geom_boxplot.html

[57] R examples. Combining boxplots and actual data points (ggplot2) [WWW]. [Retrieved 15.5.2015]. Available: http://www.zijdeman.nl/files/r_examples/boxplot_example.html

[58] Draft materials for IEC 62209-1 ed.2. Human exposure to radio frequency fields from hand-held and body-mounted wireless communication devices - Human models, instrumentation, and procedures - Part 1: Procedure to determine the specific absorption rate (SAR) for hand-held devices used in close proximity to the ear (frequency range of 300 MHz to 3 GHz). IEC MT1 for 62209. 2012-2015.

[59] Siegbahn, M.; Bit-Babik, G.; Keshvari, J.; Christ, A.; Derat, B.; Monebhurrun, V.; Penney, C.; Vogel, M.; Wittig, T., "An International Interlaboratory Comparison of Mobile Phone SAR Calculation With CAD-Based Models," Electromagnetic Compatibility, IEEE Transactions on , vol.52, no.4, pp.804,811, Nov. 2010. doi: 10.1109/TEMC.2010.2051672. Available: http://ieeexplore.ieee.org/stamp/stamp.jsp?tp=&arnumber=5555971&isnumber=5580183

APPENDIX A: PRELIMINARY RESULTS

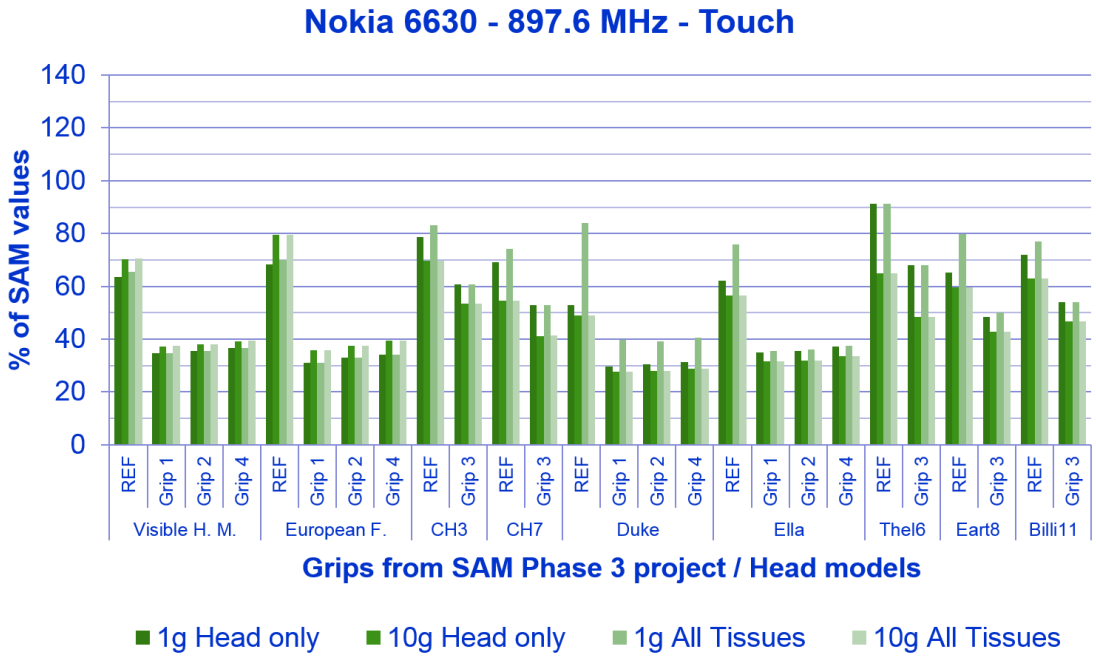

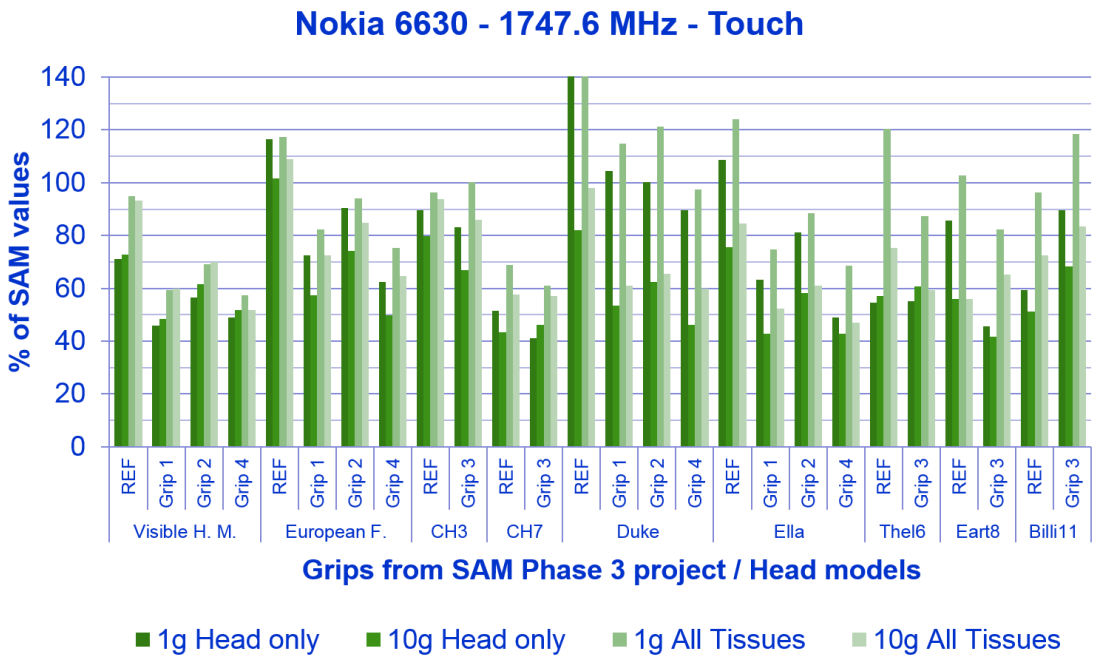

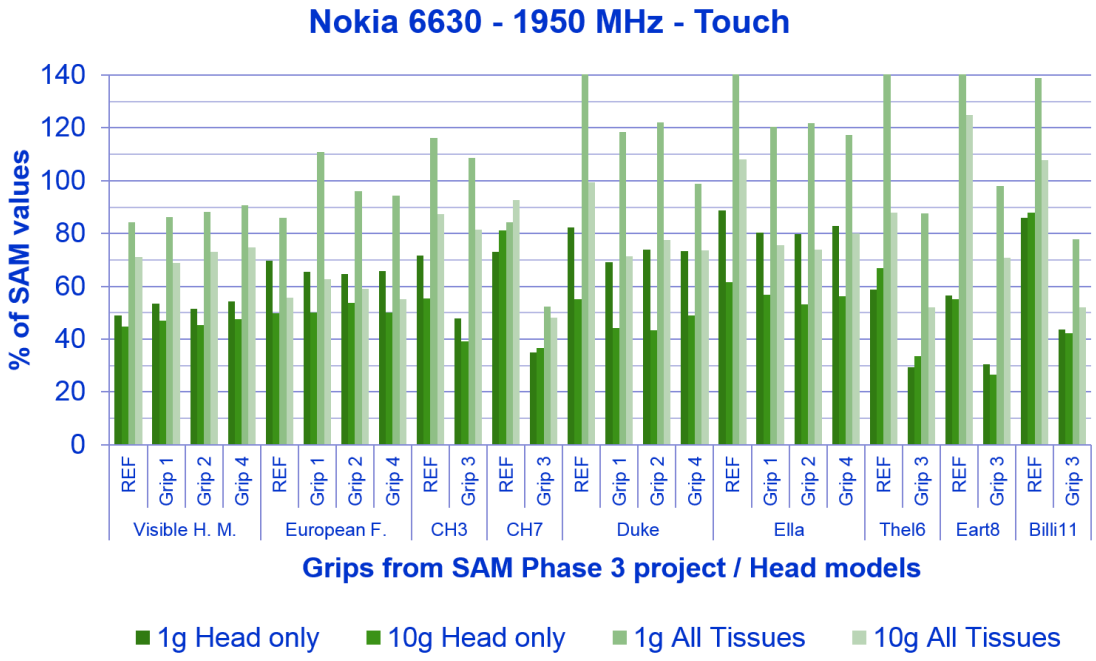
Nokia 6630 - 1950 MHz - Touch
% of SAM values
140
120
100
80
60
40
20
0
REF
Grip 1
Grip 2
Grip 4
Grip 3
Visible H. M.
European F.
CH3
CH7
Duke
Ella
Thel6
Eart8
Billi11
Grips from SAM Phase 3 project / Head models
1g Head only
10g Head only
1g All Tissues
10g All Tissues

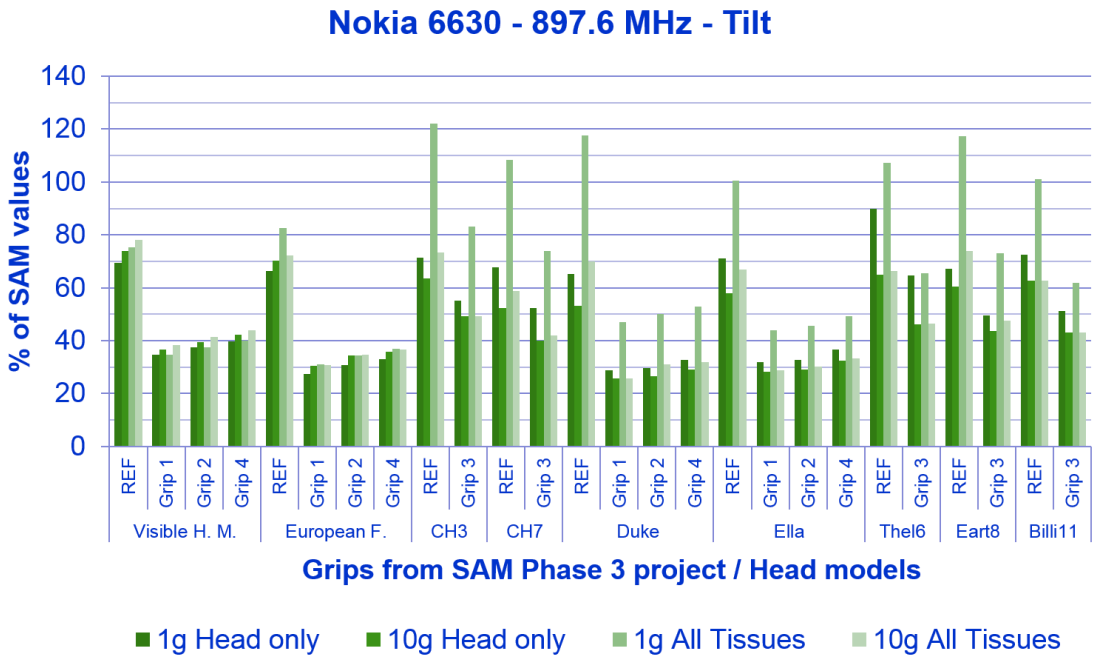
Nokia 6630 - 897.6 MHz - Tilt
% of SAM values
140
120
100
80
60
40
20
0
REF
Grip 1
Grip 2
Grip 4
Grip 3
Visible H. M.
European F.
CH3
CH7
Duke
Ella
Thel6
Eart8
Billi11
Grips from SAM Phase 3 project / Head models
1g Head only
10g Head only
1g All Tissues
10g All Tissues

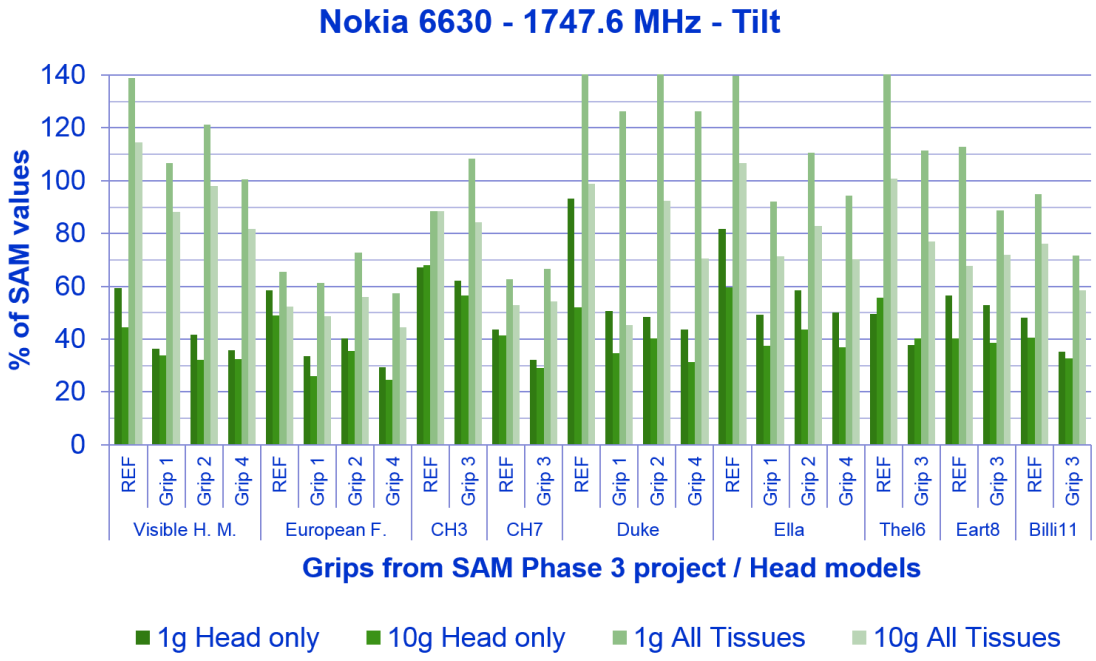
Nokia 6630 - 1747.6 MHz - Tilt
% of SAM values
140
120
100
80
60
40
20
0
REF
Grip 1
Grip 2
Grip 4
Grip 3
Visible H. M.
European F.
CH3
CH7
Duke
Ella
Thel6
Eart8
Billi11
Grips from SAM Phase 3 project / Head models
1g Head only
10g Head only
1g All Tissues
10g All Tissues

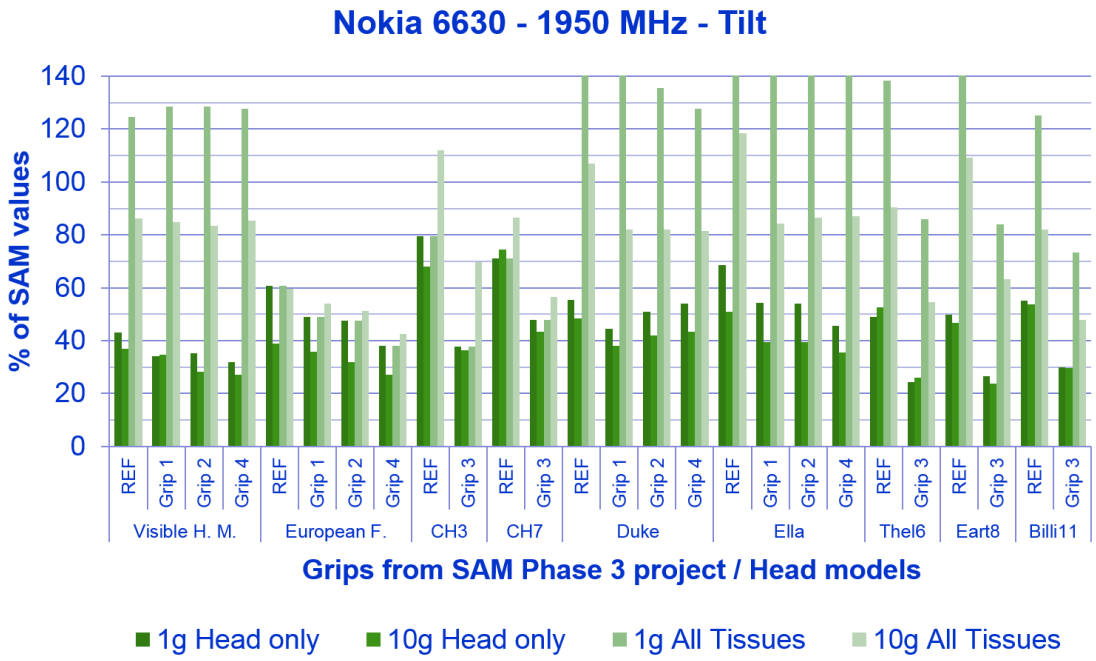
Nokia 6630 - 1950 MHz - Tilt
% of SAM values
140
120
100
80
60
40
20
0
REF
Grip 1
Grip 2
Grip 4
Grip 3
Visible H. M.
European F.
CH3
CH7
Duke
Ella
Thel6
Eart8
Billi11
Grips from SAM Phase 3 project / Head models
1g Head only
10g Head only
1g All Tissues
10g All Tissues

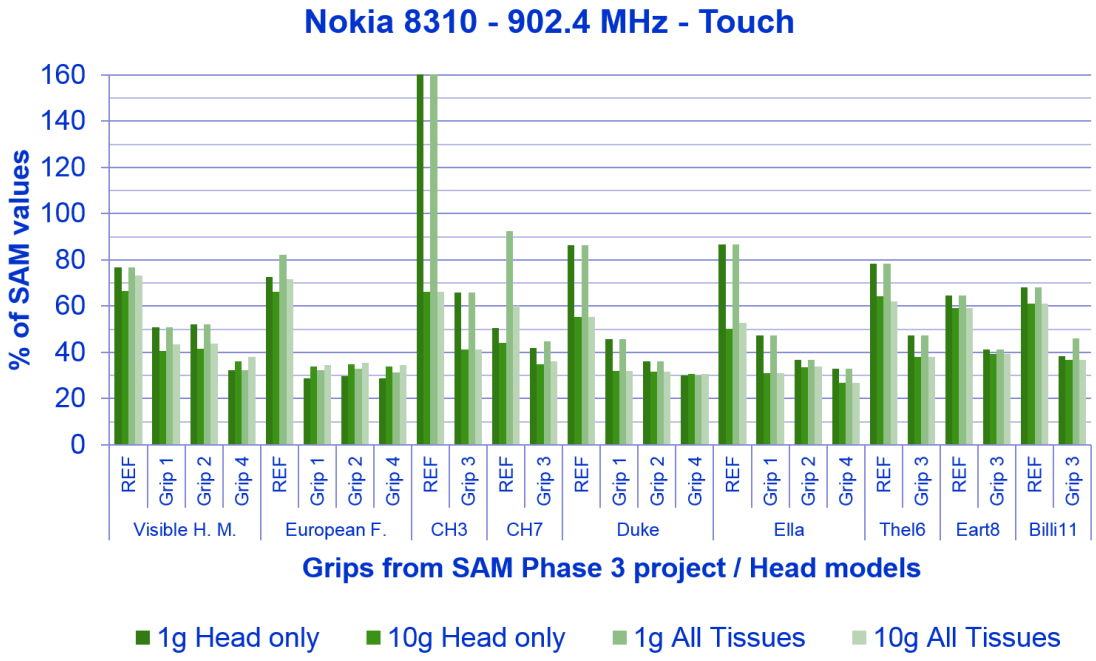
Nokia 8310 - 902.4 MHz - Touch
% of SAM values
160
140
120
100
80
60
40
20
0
REF
Grip 1
Grip 2
Grip 4
Grip 3
Visible H. M.
European F.
CH3
CH7
Duke
Ella
Thel6
Eart8
Billi11
Grips from SAM Phase 3 project / Head models
1g Head only
10g Head only
1g All Tissues
10g All Tissues

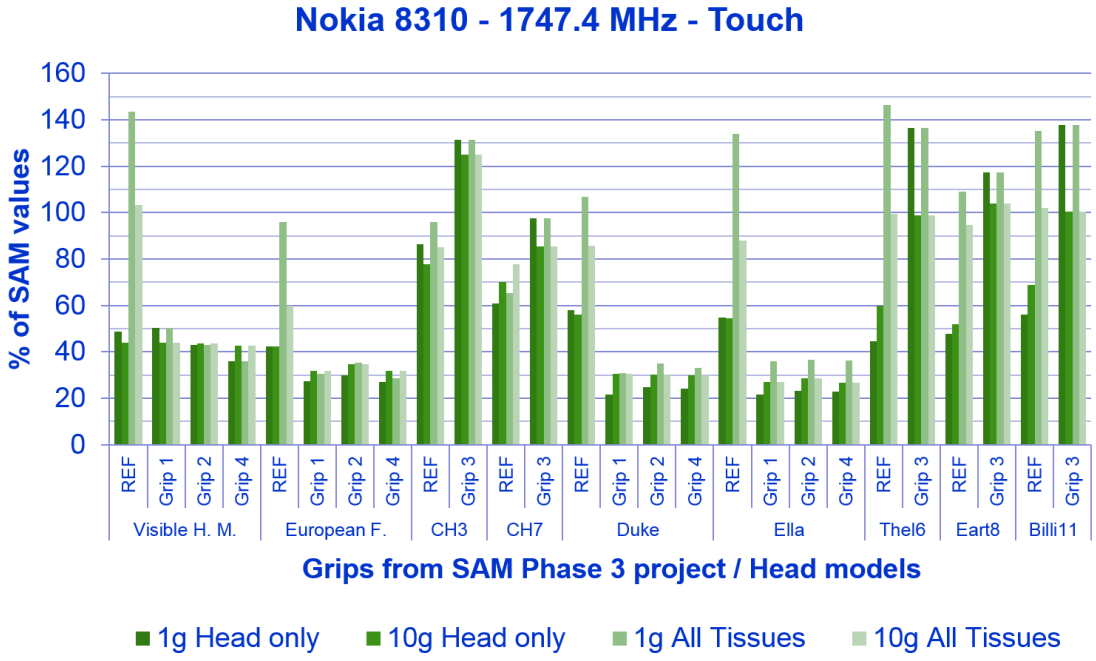
Nokia 8310 - 1747.4 MHz - Touch
% of SAM values
160
140
120
100
80
60
40
20
0
REF
Grip 1
Grip 2
Grip 4
Grip 3
Visible H. M.
European F.
CH3
CH7
Duke
Ella
Thel6
Eart8
Billi11
Grips from SAM Phase 3 project / Head models
1g Head only
10g Head only
1g All Tissues
10g All Tissues

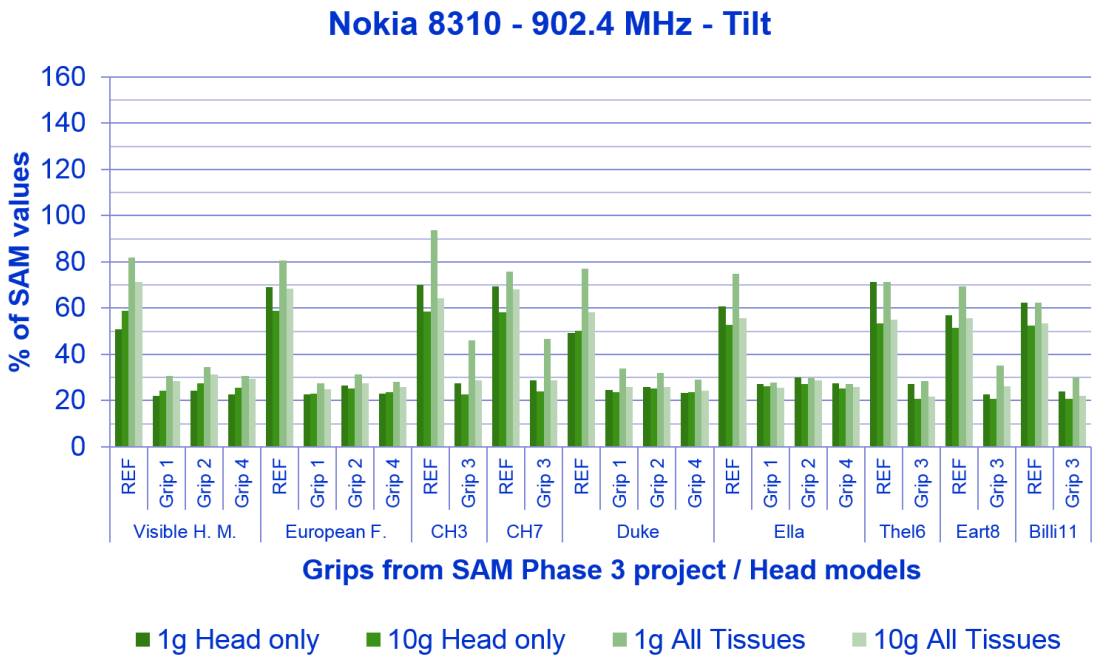
Nokia 8310 - 902.4 MHz - Tilt
% of SAM values
160
140
120
100
80
60
40
20
0
REF
Grip 1
Grip 2
Grip 4
Grip 3
Visible H. M.
European F.
CH3
CH7
Duke
Ella
Thel6
Eart8
Billi11
Grips from SAM Phase 3 project / Head models
1g Head only
10g Head only
1g All Tissues
10g All Tissues

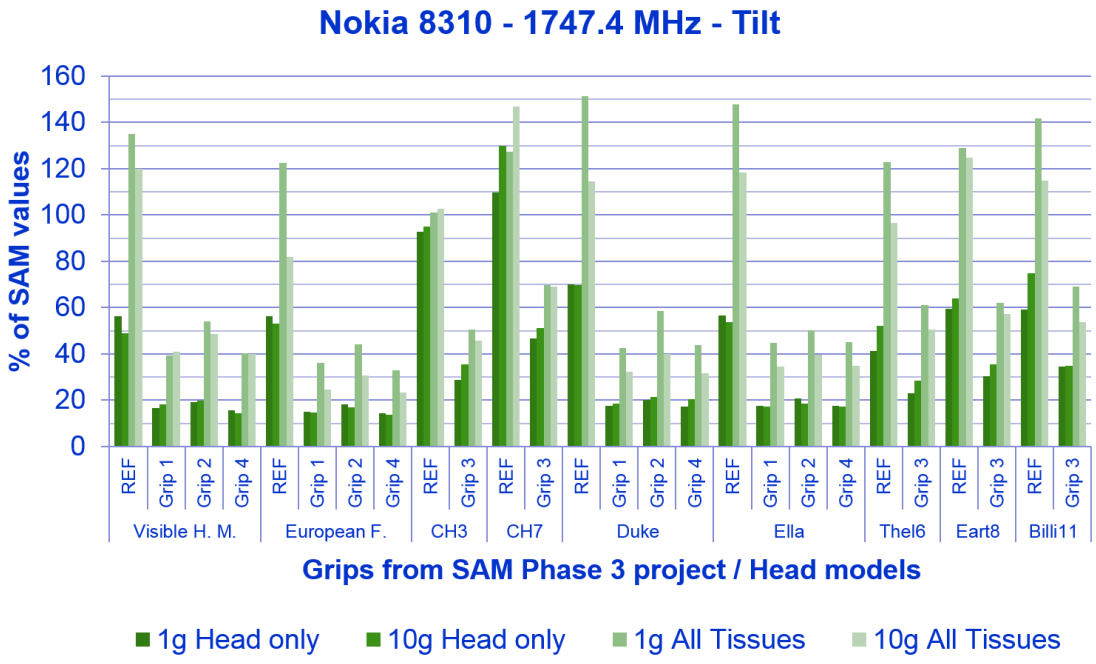
Nokia 8310 - 1747.4 MHz - Tilt
% of SAM values
160
140
120
100
80
60
40
20
0
REF
Grip 1
Grip 2
Grip 4
Grip 3
Visible H. M.
European F.
CH3
CH7
Duke
Ella
Thel6
Eart8
Billi11
Grips from SAM Phase 3 project / Head models
1g Head only
10g Head only
1g All Tissues
10g All Tissues

APPENDIX B: FINAL RESULTS

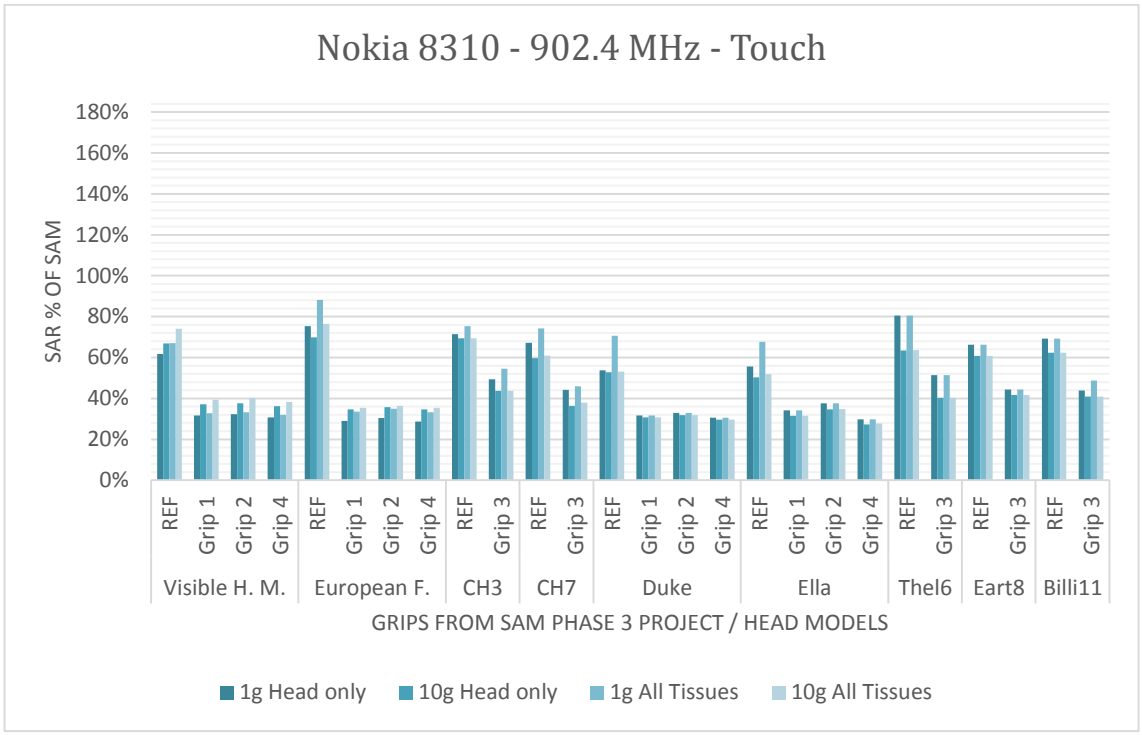

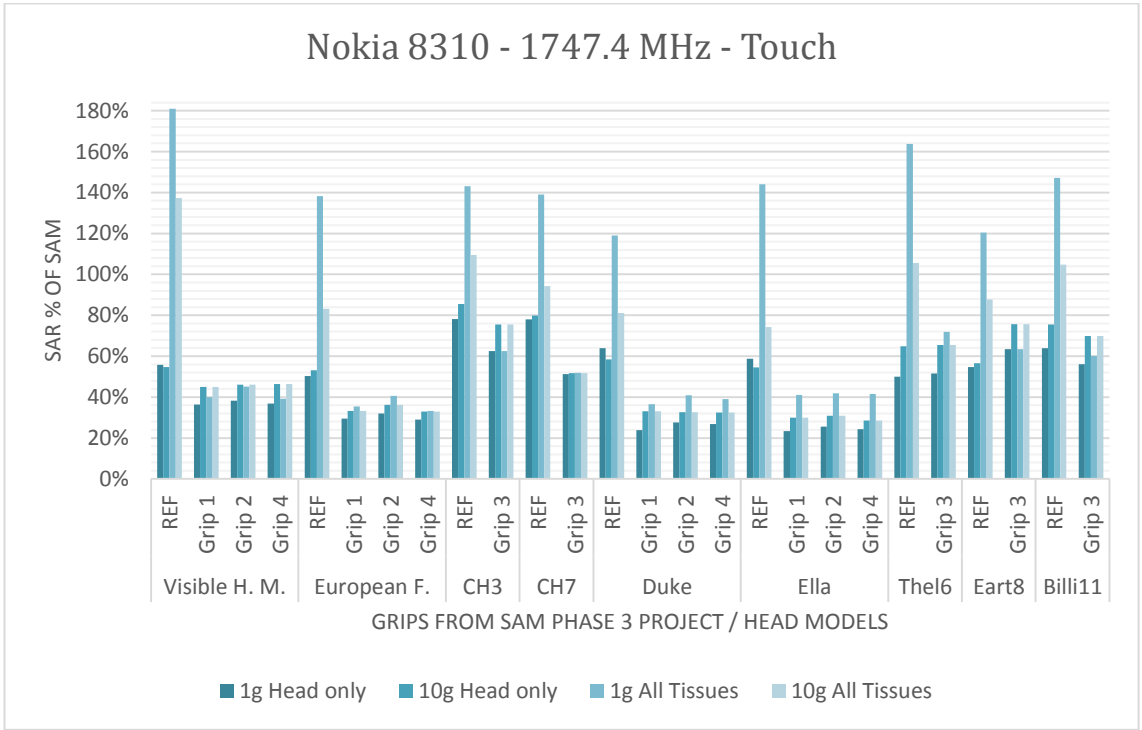

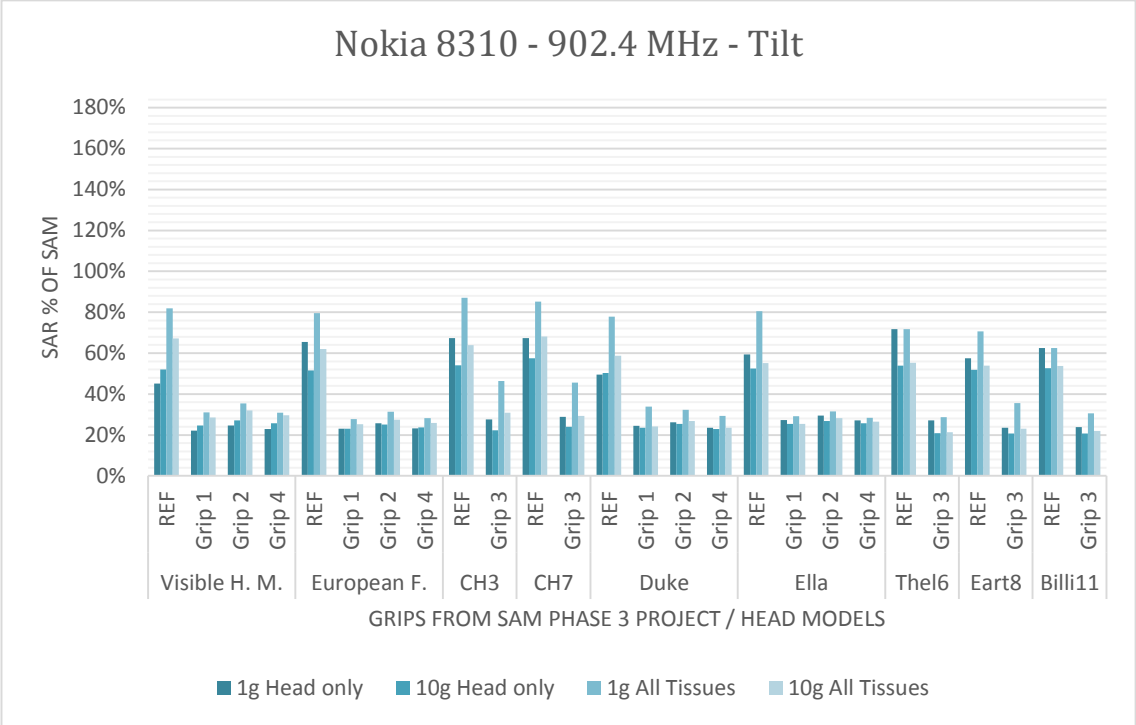
Nokia 8310 - 902.4 MHz - Tilt
SAR % OF SAM
180%
160%
140%
120%
100%
80%
60%
40%
20%
0%
REF
Grip 1
Grip 2
Grip 4
REF
Grip 1
Grip 2
Grip 4
REF
Grip 3
REF
Grip 3
REF
Grip 1
Grip 2
Grip 4
REF
Grip 1
Grip 2
Grip 4
REF
Grip 3
REF
Grip 3
REF
Grip 3
Visible H. M.
European F.
CH3
CH7
Duke
Ella
Thel6
Eart8
Billi11
GRIPS FROM SAM PHASE 3 PROJECT / HEAD MODELS
1g Head only
10g Head only
1g All Tissues
10g All Tissues

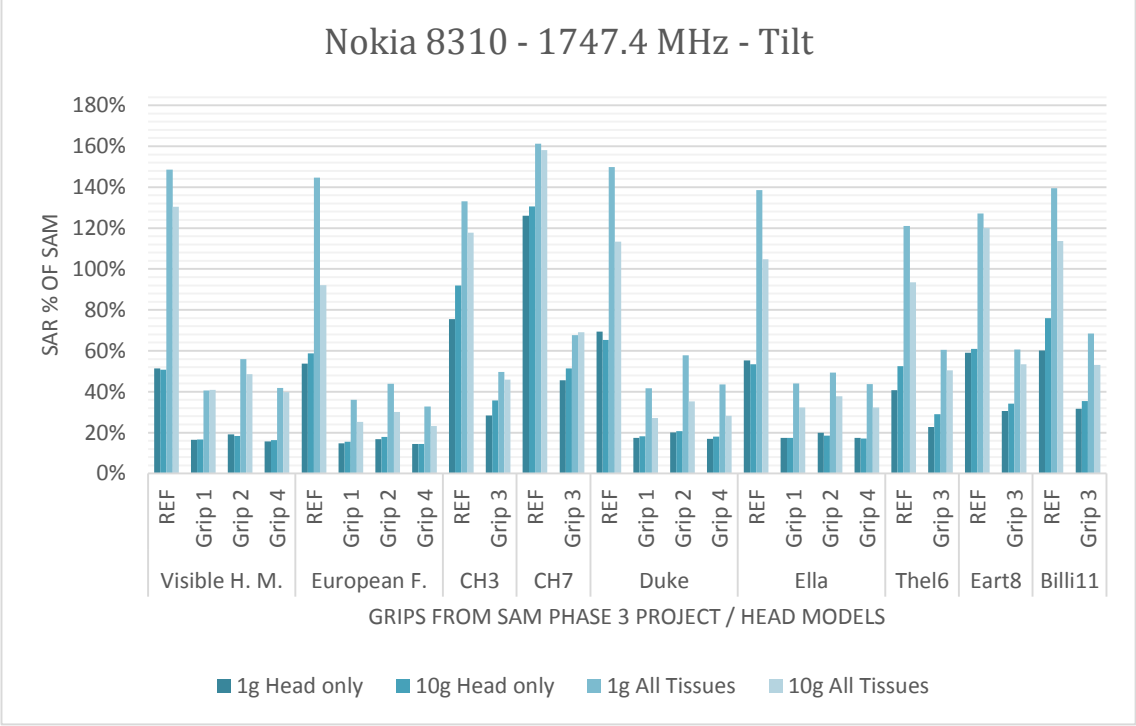
Nokia 8310 - 1747.4 MHz - Tilt
SAR % OF SAM
180%
160%
140%
120%
100%
80%
60%
40%
20%
0%
REF
Grip 1
Grip 2
Grip 4
REF
Grip 1
Grip 2
Grip 4
REF
Grip 3
REF
Grip 3
REF
Grip 1
Grip 2
Grip 4
REF
Grip 1
Grip 2
Grip 4
REF
Grip 3
REF
Grip 3
REF
Grip 3
Visible H. M.
European F.
CH3
CH7
Duke
Ella
Thel6
Eart8
Billi11
GRIPS FROM SAM PHASE 3 PROJECT / HEAD MODELS
1g Head only
10g Head only
1g All Tissues
10g All Tissues

APPENDIX C: NOKIA 8310 WITH GRIP 3 – COMPARISON

ORIGINAL 2012		
	SAR 1 g norm	**SAR 10 g norm**
8310_CH3_Grip3_902MHz_HO	6.482092	2.728071
8310_CH7_Grip3_902MHz_HO	4.121879	2.30914
8310_Thelonius_Grip3_902MHz_HO	4.673138	2.504023
8310_Eartha_Grip3_902MHz_HO	4.064884	2.593167
8310_Billie_Grip3_902MHz_HO	3.780186	2.427601
8310_CH3_Grip3_1747MHz_HO	6.884435	3.757397
8310_CH7_Grip3_1747MHz_HO	5.112044	2.572148
8310_Thelonius_Grip3_1747MHz_HO	7.162046	2.973887
8310_Eartha_Grip3_1747MHz_HO	6.153439	3.130817
8310_Billie_Grip3_1747MHz_HO	7.227906	3.019571

GRIP3 DIELECTRIC BUTTONS CORRECTION 2013				
	SAR 1 g norm	**RE SAR 1 g norm**	**SAR 1 g % orig**	**RE SAR 1 g % orig**
8310_CH3_Grip3_902MHz_HO	4.420512	4.420512	**68.19575**	**68.19575**
8310_CH7_Grip3_902MHz_HO	4.015967	4.015967	**97.4305**	**97.4305**
8310_Thelonius_Grip3_902MHz_HO	4.528052	4.528052	**96.89532**	**96.89532**
8310_Eartha_Grip3_902MHz_HO	3.965682	3.965682	**97.55953**	**97.55953**
8310_Billie_Grip3_902MHz_HO	3.667561	3.667561	**97.02065**	**97.02065**
8310_CH3_Grip3_1747MHz_HO	6.652912	4.71299	**96.637**	**68.45864**
8310_CH7_Grip3_1747MHz_HO	4.692334	4.507978	**91.78978**	**88.18348**
8310_Thelonius_Grip3_1747MHz_HO	6.701874	5.947531	**93.57485**	**83.04235**
8310_Eartha_Grip3_1747MHz_HO	5.561193	5.935812	**90.37537**	**96.46332**
8310_Billie_Grip3_1747MHz_HO	5.483544	5.414174	**75.86629**	**74.90653**
	SAR 10 g norm	**RE SAR 10 g norm**	**SAR 10 g % orig**	**RE SAR 10 g % orig**
8310_CH3_Grip3_902MHz_HO	2.607281	2.607281	**95.57231**	**95.57231**
8310_CH7_Grip3_902MHz_HO	2.23353	2.23353	**96.72563**	**96.72563**
8310_Thelonius_Grip3_902MHz_HO	2.415637	2.415637	**96.47024**	**96.47024**
8310_Eartha_Grip3_902MHz_HO	2.533365	2.533365	**97.69386**	**97.69386**
8310_Billie_Grip3_902MHz_HO	2.35082	2.35082	**96.83715**	**96.83715**
8310_CH3_Grip3_1747MHz_HO	3.538592	3.538592	**94.17669**	**94.17669**
8310_CH7_Grip3_1747MHz_HO	2.408974	2.405954	**93.65612**	**93.53873**
8310_Thelonius_Grip3_1747MHz_HO	2.974661	2.974661	**100.026**	**100.026**
8310_Eartha_Grip3_1747MHz_HO	3.134493	3.134493	**100.1174**	**100.1174**
8310_Billie_Grip3_1747MHz_HO	3.053004	3.053004	**101.1072**	**101.1072**

GRIP3 FINGER CORRECTION 2013

	SAR 1 g norm	**RE SAR 1 g norm**	**SAR 1 g % diel**	**RE SAR 1 g % diel**
8310_CH3_Grip3_902MHz_HO	4.657233	4.657233	**105.3551**	**105.3551**
8310_CH7_Grip3_902MHz_HO	4.171305	4.171305	**103.8680**	**103.8680**
8310_Thelonius_Grip3_902MHz_HO	4.855517	4.855517	**107.2319**	**107.2319**
8310_Eartha_Grip3_902MHz_HO	4.190563	4.190563	**105.6707**	**105.6707**
8310_Billie_Grip3_902MHz_HO	4.138759	4.138759	**112.8477**	**112.8477**
8310_CH3_Grip3_1747MHz_HO	2.891414	2.891414	**43.4609**	**61.3499**
8310_CH7_Grip3_1747MHz_HO	2.31985	2.364999	**49.4391**	**52.4625**
8310_Thelonius_Grip3_1747MHz_HO	2.381557	2.34787	**35.5357**	**39.4764**
8310_Eartha_Grip3_1747MHz_HO	2.934026	2.934026	**52.7589**	**49.4292**
8310_Billie_Grip3_1747MHz_HO	2.59093	2.59093	**47.2492**	**47.8546**
	SAR 10 g norm	**RE SAR 10 g norm**	**SAR 10 g % diel**	**RE SAR 10 g % diel**
8310_CH3_Grip3_902MHz_HO	2.761204	2.761204	**105.9036**	**105.9036**
8310_CH7_Grip3_902MHz_HO	2.296718	2.296718	**102.8291**	**102.8291**
8310_Thelonius_Grip3_902MHz_HO	2.545035	2.545035	**105.3567**	**105.3567**
8310_Eartha_Grip3_902MHz_HO	2.630364	2.630364	**103.8288**	**103.8288**
8310_Billie_Grip3_902MHz_HO	2.580595	2.580595	**109.7742**	**109.7742**
8310_CH3_Grip3_1747MHz_HO	2.077892	2.077892	**58.7209**	**58.7209**
8310_CH7_Grip3_1747MHz_HO	1.423474	1.423474	**59.0905**	**59.1646**
8310_Thelonius_Grip3_1747MHz_HO	1.801282	1.801282	**60.5542**	**60.5542**
8310_Eartha_Grip3_1747MHz_HO	2.08006	2.08006	**66.3603**	**66.3603**
8310_Billie_Grip3_1747MHz_HO	1.923683	1.923683	**63.0095**	**63.0095**

APPENDIX D: SAGITTAL BISECTIONS OF VOXELLED HEADS

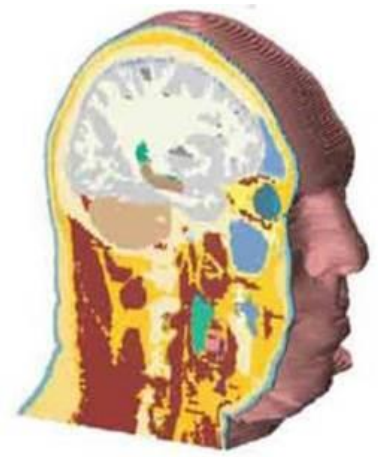

Visible Human male

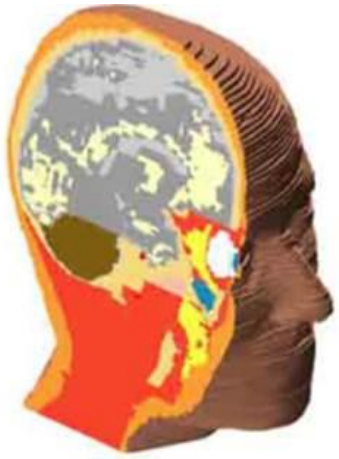

European Female

Child 7 years old

Child 3 years old

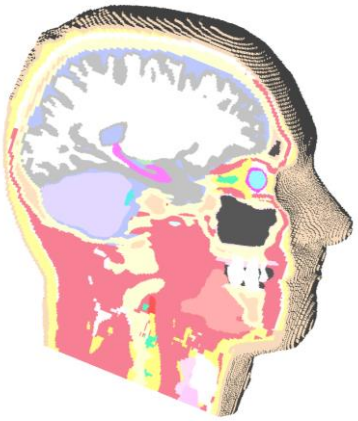

Duke

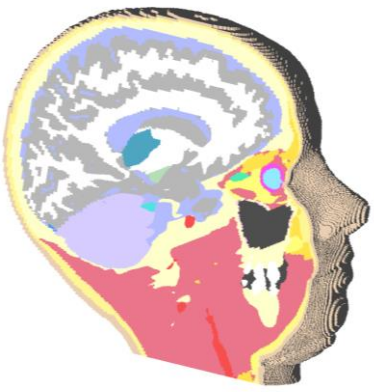

Ella

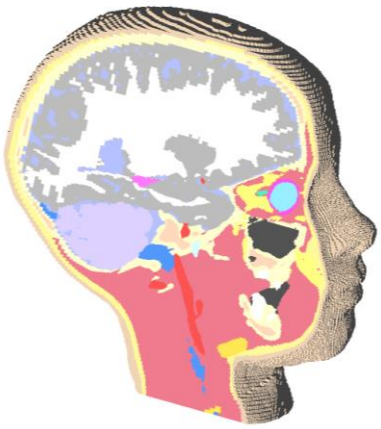

Billie

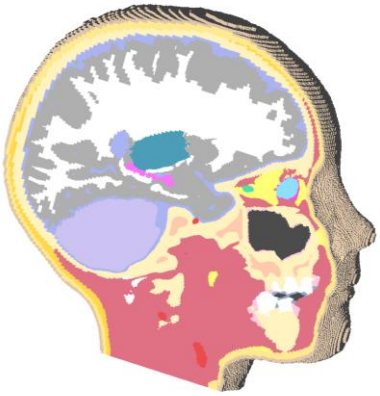

Eartha

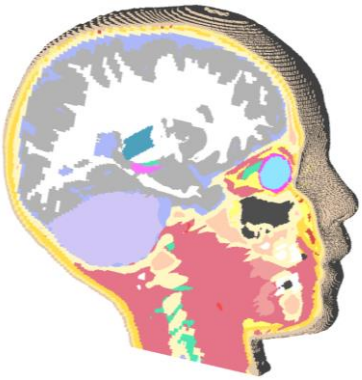

Thelonious